

École polytechnique de Louvain

# Impact of Inverter Based Generation on the Transient Stability Performance of Large Synchronous Power Plants

Author: **Ángel GARCÍA MENA**  
Supervisor: **Emmanuel DE JAEGER**  
Readers: **Bruno DEHEZ, Marc BEKEMANS**  
Academic year 2019–2020  
Master [120] in Electrical Engineering

# Preface

I would like to express my gratitude to Emmanuel for the time he dedicated to my work as supervisor as well as to all the teachers and assistants that have helped me this year.

I would also like to thank my family and friends for always being there, even in difficult times.



# Contents

<b>Preface</b> . . . . .	I
<b>Abstract</b> . . . . .	V
<b>List of Symbols</b> . . . . .	IX
<b>1 Introduction</b>	<b>1</b>
1.1 Transient behaviour of Synchronous generators . . . . .	1
1.1.1 Electromagnetic behaviour . . . . .	2
1.1.2 Mechanical Behaviour . . . . .	7
1.2 HVDC systems and DC generation . . . . .	9
1.2.1 DC generation . . . . .	9
1.2.2 HVDC Systems . . . . .	10
1.3 DC/AC Interfaces . . . . .	11
<b>2 Regulatory frame</b>	<b>13</b>
2.1 Normal operation conditions . . . . .	13
2.1.1 Reactive Power . . . . .	14
2.1.2 Active Power . . . . .	14
2.2 Faulted Conditions . . . . .	15
2.2.1 Reactive Power priority . . . . .	16
<b>3 Models Developed</b>	<b>19</b>
3.1 Elements present in the models . . . . .	20
3.1.1 Synchronous generator . . . . .	20
3.1.2 Transformers, lines and grids . . . . .	21
3.1.3 Converter . . . . .	23
3.2 Power Controls . . . . .	25
3.2.1 Reactive Power in normal operation . . . . .	25
3.2.2 Active Power in normal operation . . . . .	27
3.2.3 Control during fault situation . . . . .	28
3.2.4 Grid Configuration . . . . .	31

<b>4</b>	<b>Results</b>	<b>33</b>
4.1	Theoretical approach . . . . .	36
4.2	Experimental Results . . . . .	41
4.2.1	Three-phase fault . . . . .	42
4.2.2	Single line ground fault . . . . .	47
4.2.3	Simple Benchmark . . . . .	49
4.3	Theoretical and Experimental Comparison . . . . .	50
<b>5</b>	<b>Synchronous generator behaviour</b>	<b>55</b>
5.1	Active Power . . . . .	55
5.2	Rotor Speed . . . . .	56
5.3	Reactive Power . . . . .	57
5.4	Field Current . . . . .	58
5.5	Single Line to Ground Fault . . . . .	60
<b>6</b>	<b>Conclusions</b>	<b>63</b>
	<b>References</b>	<b>70</b>
	<b>List of figures</b>	<b>71</b>
	<b>List of tables</b>	<b>73</b>

# Abstract

This Master Thesis has one main aim: analyse the effect of the inverter based generation on the transient stability performance of large synchronous power plants.

**DC current** is starting to become more and more important in the actual electrical grid, owing to two main reasons

- Increase in DC generation sources
- Increase in use of DC for energy transport

With the aim of injecting this DC power into the electrical AC grid, an interface is needed, this interface consists in an inverter. This inverter is a controlled system, hence active and reactive power injection can be constantly and precisely regulated.

Actual increase in these kind of technologies lead to a major importance of the DC part in the electrical grid. Many researchs are being carried out for the purpose of taking advantage of the different possibilities their control offers.

On the other hand, **Synchronous machines** are the main actors in the generation process. They are directly connected to the grid so they suffer from all the different disturbances that may occur on it. Transient behaviour of these machines is crucial as it could lead to their disconnection and, so on, to major problems.

Consequently, it is noticeably important to analyse the way these DC systems and their interfaces may interact with the synchronous generators and, mainly, in the case of a large disturbance. This study is considered for both HVDC links and Power Park modules.

In order to do so, the next strategy will be followed:

Firstly, a brief theoretical introduction of the transient behaviour of the synchronous generators and the necessity and working principle of HVDC links and Power Park module,

as well as their converters, will be given, as a base for the incoming comments and results.

After that, specific european legislation about this topic and its application in the different national grid codes (Belgian and Spanish ones) will be introduced. Control requirements for both active and reactive power are presented while they are also specified the actions to be done when a large disturbance occurs.

For the normal operation conditions (when the voltage is between limits specified by the grid operator) there are different control possibilities.

- Reactive Power
  - Voltage Control Mode
  - Reactive Power Control Mode
- Active Power
  - Limited frequency sensitive mode overfrequency
  - Limited Frequency sensitive mode underfrequency
  - Frequency Sensitive mode

During a disturbance two actions possible can be applied on the inverter:

- Give priority to the reactive power injection.
- Give priority to the active power injection.

Once the general outlook has been established, different models will be developed in *Matlab/Simulink* tool. In this work, as stability studies are the main purpose, **RMS models are used for modelling the inverter**, so the DC/AC interface will be represented as three controlled current sources (one per phase).

In order to compare the effect of all the possible controls proposed in the grid codes, following four models are developed:

- **Case 1**
  - Reactive Power control in normal operation conditions: **Voltage control mode**
  - Active Power control in normal operation conditions: **Frequency sensitive mode**

- Control during the fault: **Reactive Power priority**
- **Case 2**
  - Reactive Power control in normal operation conditions: **Reference reactive power control mode**
  - Active Power control in normal operation conditions: **Frequency sensitive mode**
  - Control during the fault: **Reactive Power priority**
- **Case 3**
  - Reactive Power control in normal operation conditions: **Voltage control mode**
  - Active Power control in normal operation conditions: **Frequency sensitive mode**
  - Control Power during the fault: **Active Power priority**
- **Case 4**
  - Reactive Power control in normal operation conditions: **Voltage control mode**
  - Active Power control in normal operation conditions: **Frequency sensitive mode**
  - Control during the fault: **No Control at all**

For the purpose of validating the experimental results, they will be compared to a theoretical approach based upon voltage variations caused by the power provided during the fault. It will be done through kind of a *Superposition principle* where the whole grid is divided into two subsystems. Action of the controller is isolated on a subsystem and, assuming that the other one is invariant to the control on the converter, overall effect of each case on the voltage at the different buses can be computed through this isolated subsystem. In this way, it will be confirmed that the converter is working as it is expected to do and the results obtained from the simulations are in accordance to theoretical equations.

From these theoretical equations it can be deduced the dependency of the effect of the controllers on different parameters. Therefore, 4 cases aforementioned will be simulated for different situations regarding:

- Distance from the converter to the fault
- Distance from the converter to the synchronous generator.
- Maximum current allowed by the converter.

In addition, complexity of the benchmark where the simulation is carried out also has influence. Therefore, two benchmarks are analysed:

- **Simple benchmark:** composed of one synchronous generator, inverter, one voltage source simulating the grid and just two loads.
- **Complex benchmark:** composed of two synchronous generators (one controlled in both active power and field current and the other without any control), more loads, the inverter and two voltage sources simulating different grids.

Three-phase fault is the most critical disturbance for the stability purpose of a synchronous machine. However, it is not the most common one. Hence, effect of the controllers in the case of a SLG fault is also studied.

Finally, after obtaining the effect of the controllers on the voltage for the different situations, behaviour of several synchronous generator variables will be analysed; namely, active power, rotor speed, reactive power and field current. These effects will also be compared in the case of a controlled synchronous generator (in both turbine governor and field voltage) and a non controlled one.

Final results coming from all the simulations carried out allow to deduce that the best control option is to give priority to the reactive power during the disturbance and apply a Voltage control mode during usual working conditions. This choice lead to lower voltage dips in both generator and converter buses. Higher voltages during the fault mean higher active power injection and lower stator and field currents, what has a better transient behaviour as a consequence, allowing longer fault clearing times, giving rise to an important advantage. The larger distance from the inverter to the fault and the closer the generator to the inverter the better, as it is bigger the influence of these controls compared to a non-controlled system. In addition, it is crucial the capability of the inverter to provide reactive current during the fault, as it leads to a major influence on the system.

# List of Symbols

- $E_{d0}$ ,  $E_{d0}'$  and  $E_{d0}''$  represent the initials back electromotive forces for the  $d$  axis at steady state, the transient and the subtransient respectively.
- $E_{q0}$ ,  $E_{q0}'$  and  $E_{q0}''$  represent the initials back electromotive forces for the  $q$  axis at steady state, the transient and the subtransient respectively.
- $f$  frequency of the grid.
- $f_n$  nominal frequency of the grid.
- $i_{A,B,C}$  is the current flowing through stator phases A,B,C respectively.
- $I_{d0}$  and  $I_{q0}$  represent the prefault currents in the  $d$  and  $q$  axis respectively.
- $i_m$  represents the current associated to the stator flux linkages created by the field current.
- $I_{max}$  maximum current allowed by the converter.
- $i_{total}(0)$  represents the expression of the current associated to the whole fluxes linking the windings when the fault occurs.
- $Int$  integral action of the PI controller in the voltage control mode.
- $L_{eq}$  is the equivalent inductance of the stator for one phase.
- $P$  Active power injected by the converter.
- $P_{extra}$  extra active power to be injected during the fault when the active power is imperative.
- $P_{frequency}$  power contribution coming from the power frequency sensitive mode.
- $P_{normal}$  active power coming from the normal operation conditions active power controller.

- $P_{ref}$  reference active power set by the grid operator.
- $Prop$  Proportional action of the PI controller in the voltage control mode
- $Q$  Reactive power injected by the convert.
- $Q_{extra}$  extra reactive power to be injected during the fault when the reactive power is imperative.
- $Q_{max}$  maximum reactive current allowed by the converter during normal operation conditions.
- $Q_{normal}$  reactive power coming from the normal operation conditions reactive power controller.
- $Q_{ref}$  reference reactive power set by the grid operator.
- $R_{grid}$  resistance of the grid.
- $R_{line}$  resistance of the line
- $rt$  relation of transformation in a transformer.
- $S_{base}$  base power chosen for the converter.
- $S_n$  Nominal power
- $S_{sc}$  shortcircuit power of the grid.
- $T_a$  is the armature time constant.
- $T_d''$  subtransient time constant,  $d$  axis.
- $T_d'$  transient time constant,  $d$  axis.
- $u_{cc}$  defining the shortcircuit voltage of the transformer.
- $\vec{V} = \vec{V}_{ph-n}$  of the converter bus
- $V_d$   $d$  component of  $\vec{V}$  referred to  $\angle \vec{V}$
- $V_{1,15}$  direct sequence component of the voltage at the 15  $kV$  bus.
- $V_{2,15}$  inverse sequence component of the voltage at the 15  $kV$  bus.
- $V_{1,220}$  direct sequence component of the voltage at the 220  $kV$  bus.

- $V_{2,220}$  inverse sequence component of the voltage at the 220 kV bus.
- $V_{max1}$  lower maximum voltage limit for the fault conditions.
- $V_{max2}$  higher maximum voltage limit for the fault conditions.
- $V_{min1}$  higher minimum voltage limit for the fault conditions.
- $V_{min2}$  lower minimum voltage limit for the fault conditions.
- $V_{ph-ph}$  represents the phase to phase voltage base at the converter point.
- $V_q$   $q$  component of  $\vec{V}$  referred to  $\angle \vec{V}$
- $V_{ref}$  reference voltage for the bus where the converter is connected.
- $\Delta V_{220}$  increase of the voltage compared to the non controlled converter at 220kV bus.
- $\Delta V_{15}$  increase of the voltage compared to the non controlled converter at 15kV bus.
- $X_a$  corresponds to the flux path around the airgap.
- $X_d$  steady state reactance  $d$  axis.
- $X_d'$  transient reactance  $d$  axis.
- $X_d''$  subtransient reactance,  $d$  axis.
- $X_D$  corresponds to the flux path around the damper winding.
- $X_f$  corresponds to the flux path around the field winding.
- $X_{grid}$  reactance of the grid.
- $X_l$  corresponds to the path the armature leakage flux takes.
- $X_{line}$  reactance of the overhead line.
- $X_q$  steady state reactance  $q$  axis.
- $X_q'$  transient reactance  $q$  axis.
- $X_q''$  subtransient reactance,  $q$  axis.

## CONTENTS

---

- $\gamma_0$  represents the angle associated to the flux linkage created by the field current in phase A when the fault occurs.
- $\phi_0$  represents the angle of the current  $i_{total}(0)$  in phase A when the fault occurs.
- $\Psi_{A,B,C}$  total flux linking phase A,B,C respectively.
- $\Psi_{f,A,B,C}$  is the flux generated in phase A,B,C respectively by the field current.
- $\Psi_{A,A}$  is the flux generated in phase A by currents flowing in all the three phases. Equivalent for phases B and C.
- $\sigma$  droop for the frequency sensitive mode.
- $\cos(\varphi)$  power factor.

# Chapter 1

## Introduction

This chapter tries to give a brief explanation of the theoretical concepts that are needed for the purpose of this thesis: analyse the influence of the inverter based generation on the transient behaviour of the synchronous generators. Hence, two main topics arise, transient behaviour of the synchronous machines and working principle of inverter based generation. In order to explain them, these concepts will be addressed in three sections:

- Transient behaviour of Synchronous generators
- HVDC systems and DC generation
- DC/AC interfaces

### 1.1 Transient behaviour of Synchronous generators

Steady state working principle of synchronous machines is well known and it would take a whole chapter to explain it so, for the sake of conciseness, this section will focus on the transient performance.

It will be explained in two main parts. Firstly, main electromagnetic concepts will be introduced and the equivalent circuit for the transient period will be presented. Afterwards, active power expressions and stability problem will be addressed.

All concepts here included have been obtained through [1].

### 1.1.1 Electromagnetic behaviour

The *law of constant flux linkages* is the key concept to understand the electromagnetic phenomena that takes place in a synchronous generator when a disturbance occurs. This law states that the magnetic flux linking a closed winding cannot change instantaneously so, flux linkages just before, and just after a disturbance must be the same.

$$\Psi(t = 0^+) = \Psi(t = 0^-) \quad (1.1)$$

Based on this principle, different reactions happen depending on the kind of disturbance. In this thesis we are dealing mainly with three-phase shortcircuit and also phase to phase ones. Therefore, three-phase case will be deeply analysed and, for the sake of conciseness, just differences with the phase to phase shortcircuit will be commented.

#### Three-phase shortcircuit

According to the *law of constant flux linkages*, when a disturbance occurs the next equation shall be fulfilled.

$$\Psi_A(t) = \Psi_{AA}(t) + \Psi_{fA}(t) = \Psi_{A0} = Constant \quad (1.2)$$

$$\Psi_B(t) = \Psi_{BB}(t) + \Psi_{fB}(t) = \Psi_{B0} = Constant \quad (1.3)$$

$$\Psi_C(t) = \Psi_{CC}(t) + \Psi_{fC}(t) = \Psi_{C0} = Constant \quad (1.4)$$

Where, for each phase:

- $\Psi_A(t)$  is the total flux linking phase A
- $\Psi_{AA}(t)$  is the flux generated in phase A by currents flowing in all the three phases.
- $\Psi_{fA}(t) = \Psi_f \cdot \cos(\omega t)$  is the flux generated in phase A by the field current.
- $\Psi_{A0}$  is the total flux linking phase A at the moment of the fault.

Therefore, based upon the previous equations and provided that the equivalent inductance of each of the phase windings is the same and does not depend on the rotor position, current in each phase can be expressed as  $i_a(t) = \frac{\Psi_{AA}(t)}{L_{eq}}$ .

Final general expressions for each phase current are:

$$i_A(t) = -i_m(t) \cdot \cos(\omega t + \gamma_0) + i_{total}(0) \cdot e^{-t/T_a} \cdot \cos(\phi_0) \quad (1.5)$$

$$i_B(t) = -i_m(t) \cdot \cos(\omega t + \gamma_0 - 2\pi/3) + i_{total}(0) \cdot e^{-t/T_a} \cdot \cos(\phi_0 - 2\pi/3) \quad (1.6)$$

$$i_C(t) = -i_m(t) \cdot \cos(\omega t + \gamma_0 + 2\pi/3) + i_{total}(0) \cdot e^{-t/T_a} \cdot \cos(\phi_0 + 2\pi/3) \quad (1.7)$$

Where:

- $i_m(t)$  represents the current associated to the stator flux linkages created by the field current.
- $\gamma_0$  represents the angle associated to the flux linkage created by the field current in phase A when the fault occurs.
- $i_{total}(0)$  represents the expression of the current associated to the whole fluxes linking the windings when the fault occurs.
- $\phi_0$  represents the angle of the current  $i_{total}(0)$  in phase A when the fault occurs.
- $T_a$  is the armature time constant, representing the energy dissipation in the stator resistance.

As it can be seen, current in each phase is composed of two parts, an AC component and a DC one. These currents are going to create two mmf reactions. The AC phase currents will induce a rotating mmf, however, as the rotor is spinning at the same frequency than the one of these, it is perceived as a stationary force. On the other hand, DC stator component will create a stationary mmf, seen from the rotor as a alternating one, rotating at the synchronous speed.

Therefore, as constant flux linkage principle is also valid for rotor windings (and core), these magnetomotive forces (translated in fluxes) will induce additional rotor currents. It can be said, that there is always a complementary pair of stator to rotor currents of the form AC  $\rightarrow$  DC and DC  $\rightarrow$  AC.

DC currents both in the rotor and in the stator try to keep the flux linkages constant and equal to their pre-fault values. However, as resistances are present in both structures, there is an energy dissipation which provokes the DC currents to vanish, which is represented in the stator currents by the armature time constant  $T_a$  in eqs. 1.5, 1.6 and 1.7.

This effect has two consequences in the stator circuit during the transient period:

- Different Armature flux paths.
- Different Emf values.

What lead to the variant amplitude of the AC component in the stator currents,  $i_m(t)$  in eqs. 1.5, 1.6 and 1.7.

**Armature flux paths** It is proper to analyse this effect in the quadrature axis ( $d$  and  $q$ ), different situations occur for each of them.

From now on a synchronous machine with one damper winding in the  $d$  axis and another one in the  $q$  axis is going to be considered.

Elements present in the  $d$  **axis** are the field winding and the damper one. Therefore, each of them try to keep constant the flux across it. It can be explained as if the "new" flux coming from the armature windings could not penetrate these windings and was forced outside them, which means going through the airgap instead of the iron, giving place to a higher reluctance path and a lower reactance. This effect endure as long as the damper and field fluxes remain equal to their prefault value. As mentioned above, these fluxes decrease with the time constants defined by their electrical circuits. Damper winding has a lower time constant than the field one. Hence, three different states are going to be considered:

- Subtransient state: fluxes across both damper and field windings are equal to their prefault values. Defined by  $T_d''$  time constant.
- Transient state: only the flux across the field winding is equal to its prefault value. Defined by  $T_d'$  time constant.
- Steady state: screening effect of both windings dissappear.

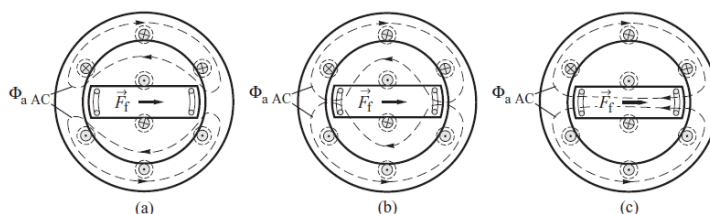


Figure 1.1: Armature flux paths in the different transient states, (a) subtransient, (b) transient, (c) steady state

Figure 1.1 shows an schematic view of the magnetic paths for the armature flux during the different states of the transient. These paths are represented through different armature reactances,  $X_d''$ ,  $X_d'$  and  $X_d$ , which are shown in Figure 1.2.

Where:

- $X_D$  corresponds to the flux path around the damper winding.
- $X_l$  corresponds to the path the armature leakage flux takes.

- $X_f$  corresponds to the flux path around the field winding.
- $X_a$  corresponds to the flux path around the airgap.

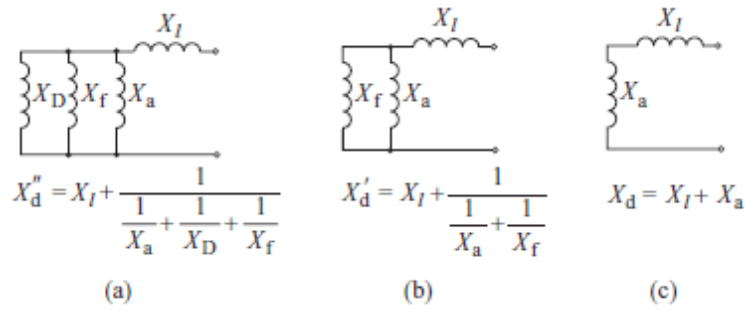


Figure 1.2: Armature reactances in the different transient states, (a) subtransient, (b) transient, (c) steady state

For the  $q$  **axis** same principle occurs. However, there is no field winding in this axis, so rotor screening effect will come from the damper winding located in this axis and from the core eddy currents (if the rotor is laminated they would be too low).

Therefore, for this case where damper winding is present in the  $q$  axis,  $X_q'' \approx X_d''$ , if the machine is composed of a round rotor some screening effect will be present in the transient state, hence,  $X_q' \approx 2X_d'$ . In addition, for the steady state and a round rotor generator,  $X_q \approx X_d$  as there is always some saliency present.

### Emf values

Based on the same principle of constant flux linkages. Flux linking the stator and coming from the rotor, which give place to the back electromotive force, is varying during the transient. Hence, Emf values are also changing.

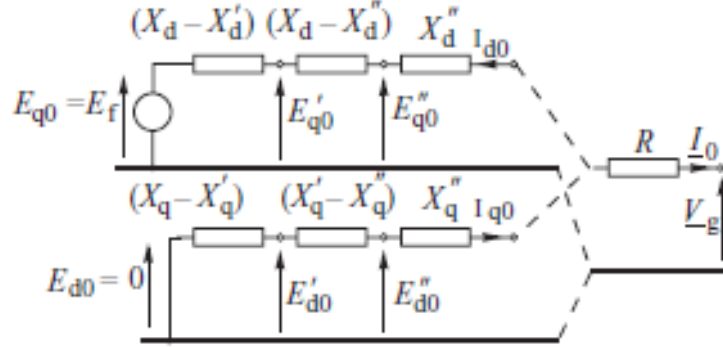


Figure 1.3: Emf in the different transient states

Where:

- $E_{d0}$ ,  $E_{d0}'$  and  $E_{d0}''$  represent the initials back electromotive forces for the  $d$  axis at steady state, the transient and the subtransient respectively.
- $E_{q0}$ ,  $E_{q0}'$  and  $E_{q0}''$  represent the initials back electromotive forces for the  $q$  axis at steady state, the transient and the subtransient respectively.
- $I_{d0}$  and  $I_{q0}$  represent the prefault currents in the  $d$  and  $q$  axis respectively.

Figure 1.3 represents this situation. For the  $d$  axis, flux linking the rotor in the prefault situation is equal to the one generated by the field current minus the one coming from the stator ones while for  $q$  axis, as there is no source of flux placed at the rotor in this direction, flux linking the rotor is just equal to the one generated by the stator currents.

$$\Psi_{rotord,prefault} = \Psi_f - I_{d0} \cdot X_d \quad (1.8)$$

$$\Psi_{rotorq,prefault} = I_{q0} \cdot X_q \quad (1.9)$$

Minus sign for the  $d$  axis and positive for the  $q$  one is just a sign convention expressing that the flux generated by stator currents is opposite to the field one and it is positive for current in the  $q$  axis in the normal operation conditions of the generator.

This flux is kept constant during the subtransient state and it becomes the total flux generated by the rotor linking the stator, giving place to  $E_{q0}''$  and  $E_{d0}''$ . During the transient state this flux linking the stator decreases, as damper windings stop producing this flux. This flux variation linking the stator give place to  $E_{q0}'$  and  $E_{d0}'$  and it is expressed as:

$$\Delta \Psi_d = -I_{d0}(L_d' - L_d'') \quad (1.10)$$

$$\Delta\Psi_q = I_{q0}(L_q' - L_q'') \quad (1.11)$$

Same phenomena occurs for the steady state, where the total flux generated by the rotor and linking the stator is again just the produced by the field current.

With all these concepts and expressions it is possible to build the equivalent circuit for each state and obtain all the electrical variables.

### Phase to phase shortcircuit

For the case of a phase to phase shortcircuit, as it is known, currents flowing in the stator are assymmetrical, meaning that they generate an mmf spatial vector which is composed of an inverse sequence component, appart from the DC and the direct sequences components present in the three-phase shortcircuit.

Hence, the reasoning for obtaining the final electrical circuit and variables during the transient is the same that for the case of a three-phase shortcircuit but adding the effect of the inverse sequence component.

### 1.1.2 Mechanical Behaviour

Now, it is time to explain how the shaft behaves during this period and the constraints that shall be fulfilled in order to reach the stability once the fault is cleared.

In order to do so, it is important to obtain the expression for the electrical power injected during the fault and, by comparing it with the mechanical input power, study the mechanical behaviour of the rotor.

As explained before, during the transient period, different back electromotive forces are induced in the stator. It is necessary to choose one of these values, as the subtransient period is usually very short compared with the period of the rotor swings, the effect of the subtransient phenomena on the electromechanical dynamics can be neglected. This allows the use of  $E'$ .

Assuming that  $X_d' \approx X_q'$ :

$$P_e = \frac{E'V_s}{X_{total}} \sin(\delta') \quad (1.12)$$

Where:

- $V_s$  is the voltage of the grid where the power is being injected.

- $X_{total}'$  is the value of the reactance linking the generator and the grid.
- $\delta'$  is the angle between  $E'$  and  $V_s$ .

$X_{total}'$  can be divided into prefault, fault and postfault values. If the fault is cleared with no change in the grid, pre and postfault values are equal. If a three phase fault occurs at one line at the generator bus  $X_{total,fault}' = \infty$ .

This situation ( $X_{total,fault}' = \infty$ ) can be represented in figure 1.4.  $P_{E'}(\delta')$  represents the electrical power injected to the grid in the prefault situation,  $P_m$  represents the mechanical power injected to the shaft (it is supposed to remain constant during the transient) and the electrical power injected during the fault is equal to zero.

At point 1 the fault occurs, the electrical power goes to zero. Therefore, as long as the fault is present, there is an excess of input power in the system what leads to an acceleration of the rotor. Increase in mechanical energy is equal to the surface defined by points 1 to 4. Once the fault is cleared active power is again injected, its value is bigger than the mechanical power so the rotor decelerates, once all the extra energy stored during the fault has been released (surface defined by points 4 to 7) the rotor starts to swing around its stable value until it finally reaches it.

Last concept explained above is the *equal area criterion*. If the fault would be present for a longer time, during the "recovery" period, electrical power could go beyond point 8. If this happens, electrical power would be again lower than the mechanical one so the rotor would accelerate and the system would be unstable.

Clearing time is therefore a essential in stability studies. *Critical clearing time* is the longest clearing time for which the generator will remain in synchronism.

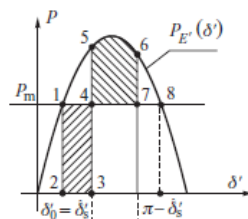


Figure 1.4: Active power balance in a three-phase fault close to the generator

As it can be deduced, the place where the fault occurs is a crucial parameter, as it directly

affects the  $X_{total,fault}$  parameter and allow higher power injections.

Related with this  $X_{total,fault}$  parameter is the kind of fault that occurs in the system. Previous comments were based upon a three-phase fault case. However, in the case of other large disturbances,  $P_{E'}(\delta')$  during the fault has different values, as healthy phases may be available for the active power transmission purpose. This effect can be observed in figure 1.5.

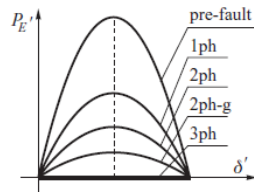


Figure 1.5:  $P_{E'}(\delta')$  depending on the kind of fault, when close to the generator

## 1.2 HVDC systems and DC generation

DC current is becoming more and more important in the actual electrical grid. This is due to two main reasons. Increase in the amount of sources generating in DC and the increase of DC used for transmitting power along the grid. A brief explanation of both reasons will be given in order to understand the necessity of carrying out studies for analysing the effect of this new grid feature in the behaviour of synchronous generators, which is the aim of this thesis.

### 1.2.1 DC generation

Traditional generation sources give place to AC voltages and currents flowing in the stator. However, increase in the share of renewable energies in the energy mix [2] lead to a change in this statement, as most of them are linked somehow to DC current.

Due to the working principle of the solar cells they are composed of, *Photovoltaic* panels produce DC current. This technology is the one leading the increase in renewable energies [2] so it shall be taken into account.

Notwithstanding other renewable sources (wind energy, hydropower) directly obtain the energy from the different natural resources in AC, they need a DC interface for one main

technical purpose [3]:

**Control the electromagnetic torque** exerted on the mechanical shaft in order to extract the maximum power: due to fluid dynamics concepts, in order to absorb the maximum amount of power, speed of the shaft must be adapted to the speed of the natural resource they are taking advantage of. This is mainly done for wind energy systems. For the purpose of controlling the rotor speed, managing the electromagnetic torque exerted on the shaft is the most common strategy. This consists in injecting the desired currents in the electrical machine, what needs from a DC block in order to apply the needed voltages for inducing the calculated currents.

### 1.2.2 HVDC Systems

HVDC transmission systems are expected to increase during the coming years (reference), they are used as flexible transmission systems and they offer a variety of advantages compared to AC ones [4]:

- Flexible approach of mutual support and supply security in interconnected systems.
- Better integration of renewable energies
- Contribution to better flexibility management.
- Facilitation of energy markets.
- Lower corona and capacitive effect compared to long AC cables.
- No Skin effect.
- Better voltage control and stability compared to AC systems.
- Lower costs compared to the AC transmission system above a certain distance.

As an example, figure 1.6 shows the decrease in the costs above a certain distance.

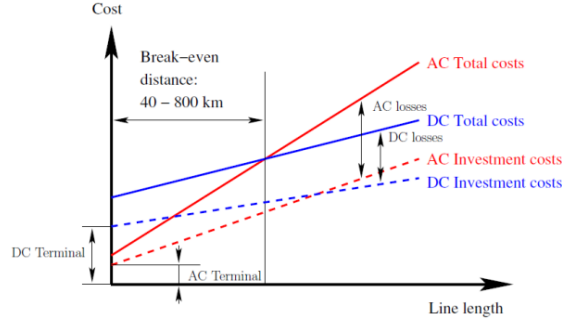


Figure 1.6: Comparison of costs for HVDC and AC transmission systems in function of the distance

### 1.3 DC/AC Interfaces

As mentioned above, in order to inject the power coming from DC links in the electrical grid it is necessary to transform it into AC. In order to do so an inverter is used. Most common kind of inverters for this purpose are:

- Line commutated converters.
- Voltage source converters.

Voltage source converters are the most commonly used nowadays. Inverter connecting the DC bus with the AC grid is controlled in such a way that can manage the amount of active and reactive power injected. This is done in the following way [4].

$$P = \frac{V_{a,c} V_{V_{sc}} \sin \theta}{X} \quad (1.13)$$

$$Q = \frac{V_{a,c} [V_{V_{sc}} \cos \theta - V_{a,c}]}{X} \quad (1.14)$$

Where:

- $V_{a,c}$  is the voltage amplitude of the electrical grid.
- $V_{V_{sc}}$  is the voltage amplitude of the output of the inverter.
- $\theta$  is the angle between the two voltages variables.
- $X$  is the impedance placed for connecting the converter and the grid (otherwise it would not be possible to connect the converter, as two voltage sources would be placed in parallel).

$V_{a,c}$  and its phase are measured continuously and the impedance  $X$  is also known. Therefore, by setting the proper voltage in the output of the converter (amplitude and phase) desired power can be obtained. In order to make easier the calculation it is done in the  $d, q$  frame. Resultant values are transformed into  $abc$  frame and are applied through a controlled inverter. Methodology followed is the one shown in figure 1.7.

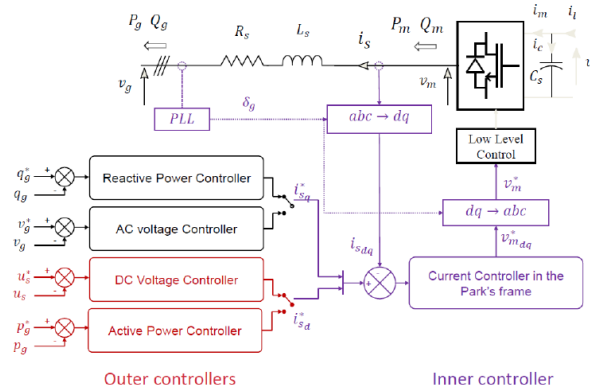


Figure 1.7: Control strategy applied in a Voltage source inverter

As it is shown, active power can be controlled in order to keep the voltage constant at the DC bus. In addition, instead of injecting a reference value for the reactive power, it might be chosen to control the amplitude of the AC voltage, acting in a voltage control mode.

All the elements related to the aim of this thesis have been now theoretically introduced. For the purpose of analysing the influence of inverter based generation (and HVDC links) in the transient behaviour of the synchronous machines, different control strategies will be applied to their DC/AC interface in order to see the most advantageous ways to keep synchronous machines stable after a large disturbance and, if possible, increase crucial parameters as the critical clearing time.

# Chapter 2

## Regulatory frame

It is important to note that DC power connection to the grid is an important and actual topic. Therefore, specific requirements have been established. These requirements are set by *The European Commission "for grid connection of high voltage direct current systems and direct current-connected power park modules"* [5] and are applied by national Grid Operators of each country in particular.

In this thesis two national grid codes are studied, the Spanish [6] and the Belgian [7] ones. Both documents are really similar, however, Spanish requirements is the one used as they give some more specific information.

Most interesting parts for the aim of this thesis are:

- Active and Reactive Power Control Modes during "normal" operation conditions.
- Actions to be done in the case of a disturbance.

### 2.1 Normal operation conditions

Normal operation conditions refer to the situation when the voltage at the connection point of the DC system is between a certain margin around the reference value (1 pu).

$$V \leq V_{max1} \tag{2.1}$$

$$V \geq V_{min1} \tag{2.2}$$

Where, usually,  $0.85 \leq V_{min1} \leq 0.9pu$  and  $1.05 \leq V_{max1} \leq 1.1pu$ .

### 2.1.1 Reactive Power

For the reactive power two main controls are addressed:

- **Reactive Power Control Mode:** this mode refers to the case where the reactive power that shall be injected is set to a constant reference value that must be achieved.
- **Voltage Control Mode:** this mode refers to the case where the reactive power injected varies according to the value of the voltage at the connection point of the converter, compared to a reference one. If the voltage is below the reference, more reactive power is injected. Otherwise, if it is above, reactive power is reduced. Concerning the maximum instantaneous change in the reactive power, it is specified that  $\Delta Q \leq 0.3\% Q_{max}$  for an  $\Delta V = 1kV$ .

For both controls, one minimum operation area is specified. This is done with respect to the maximum active power capability and is shown in Figure 2.1. Area inside dashed lines show the most common operation voltages, however, the system shall be capable of providing reactive power in the top and bottom regions at the maximum active power production.

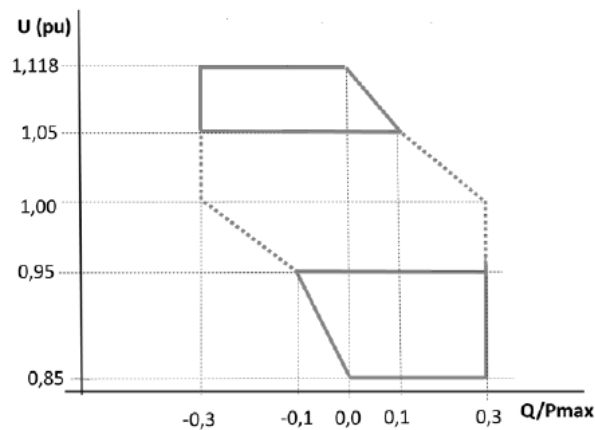


Figure 2.1: Reactive Power capability in extreme voltage ranges

### 2.1.2 Active Power

For the active power, output shall **follow the reference value specified by the grid operator**. In addition, the grid operator may ask the owner of the system to be able to react against frequency deviations. This frequency response can be classified among three different types:

- **Limited frequency sensitive mode overfrequency:** the system reacts only when the frequency is above a certain threshold.
- **Limited frequency sensitive mode underfrequency:** the system reacts only when the frequency is below a certain threshold.
- **Frequency sensitive mode:** the system reacts to both over and underfrequency phenomena.

Frequency response shall be summed up to the active power reference value specified by the grid operator.

Scheme of the control action for the case of frequency sensitive mode is plot in Figure 2.2 and different parameters regarding its operations conditions in Figure 2.3.

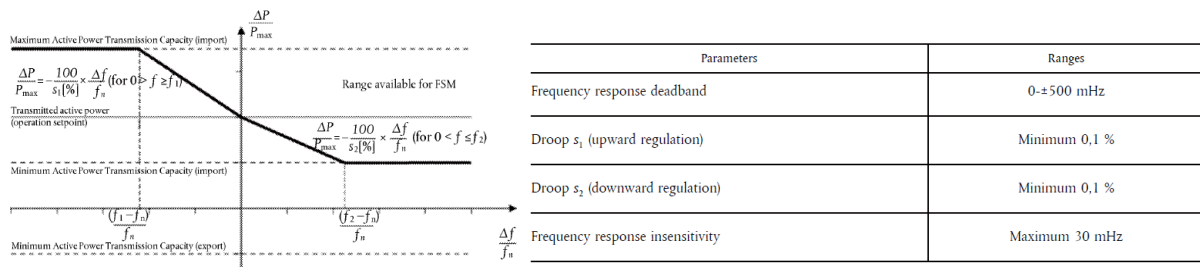


Figure 2.2: Frequency sensitive mode scheme      Figure 2.3: Frequency sensitive mode parameters

## 2.2 Faulted Conditions

This situation is considered when:

$$V > V_{max1} \quad \text{or} \quad V < V_{min1} \quad (2.3)$$

Where  $V_{max1}$  and  $V_{min1}$  are the same values than the ones specified for the normal operation conditions case.

Ways to control the active and reactive power depends on the priority principle set in the system. European comission relinquish this responsability to national grid operators. Spanish and Belgian ones give priority to the reactive power, and does not mention how to deal with active power priority case. Therefore, first case will be the one here explained.

### 2.2.1 Reactive Power priority

This methodology specifies that in the case of a fault (verified through voltage conditions, eq. 2.2) reactive current shall be injected primarily and active power injection relies on the amount of this reactive current.

Reactive current injected is the contribution of two terms:

- Reactive current from the normal operation conditions control.
- Additional reactive current dependent on the voltage deviation.

For symmetrical faults this additional current injected due to the large voltage deviation (above the minimum limits) shall be proportional to the difference between the real value and the limit which is being exceeded. This relationship remains until the maximum current allowed by the converter is achieved, this situation must be reached when the voltage gets equal to  $V_{min2}$  or  $V_{max2}$  depending on the under or over voltage situation, respectively. This situation is graphically explained in figure 2.4.

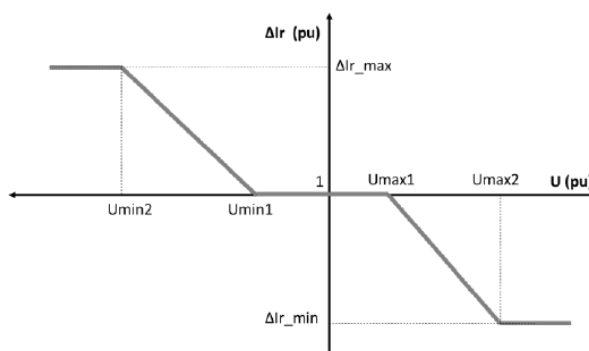


Figure 2.4: Additional reactive current when reactive power is imperative

Where, usually:

$$1.1 \leq V_{max2} \leq 1.4pu \quad \text{or} \quad 0.6 \leq V_{min2} \leq 0.85pu \quad (2.4)$$

Maximum current (total contribution) shall be at least  $I_{max} = 1pu$  (in the base frame of the converter) and higher if it is allowed.

If current limit is not achieved (when the voltage is between  $limit_1$  and  $limit_2$ ) active power will be injected up to the total current limit.

For the case of unsymmetrical faults, similar controls must be applied, however, direct or inverse currents could be injected/absorbed.

With respect to this faulty situation strict time limits are established:

- Response time since the voltage deviation occurs up to reactive current starts to be injected must be lower than 20 *ms*.
- Response time since the beginning of the reactive current injection until 90% of the final expected current is reached shall be lower than 30 *ms*.
- Response time since the start of the reactive current injection until it remains between  $\pm 5\%$  of the final expected current cannot exceed 60 *ms*.



# Chapter 3

## Models Developed

In this work, many models are studied in order to analyse the differences among the different kinds of controls previously presented. These models can be classified attending to diverse features:

- **Control for the reactive power during normal operation conditions**
  - Reference reactive power control mode
  - Voltage control mode
- **Control for the active power during normal operation conditions**
  - Frequency sensitive mode
  - Limited frequency sensitive mode overfrequency
  - Limited Frequency sensitive mode underfrequency
- **Control during fault situations**
  - Give priority to active power
  - Give priority to the reactive power
  - No Control at all
- **Grid Benchmark**
  - Simple benchmark
  - Complex benchmark

In order to make a good explanation of these models, as a first step all the elements used in the grid will be presented. After that, the different control strategies applied on the converter will be detailed. Finally, schemes of the different benchmark used will be shown.

## 3.1 Elements present in the models

For the purpose of this thesis most important parts are the synchronous generator and the DC/AC converter. However, other components are needed in order to connect them and make the final models realistic. All of them will be now detailed.

### 3.1.1 Synchronous generator

Synchronous generator analysed in this thesis is modelled by the "Synchronous machine pu fundamental" *Matlab/Simulink* block. Following main features have been set:

- 15 *kV*, 600*MVA* Round rotor machine with two pairs of poles.
- Two damper windings, one in the *d* axis and another in the *q* one.
- Voltage Control, "Excitation system IEE type 1" block defined by a regulator gain  $K_a = 10$  and a time constant  $T_a = 0.001$  *s*.
- Active Power control, "Hydraulic turbine and governor" block defined by a servomotor with a gain  $K_a = 10/3$  and a time constant  $T_a = 0.07$  *s*.

Most important parameters about transient behaviour can be seen in Table 3.1, which were obtained from [1].

$X_d$	$X_d'$	$X_d''$	$X_q$	$X_q'$	$X_q''$	$X_l$	$T_d'$	$T_d''$	$T_q'$	$T_q''$
2	0.39	0.28	1.85	0.52	0.32	0.1	0.85	0.028	0.58	0.058

Table 3.1: Generator Parameters

As it can be noticed, despite the fact that a round rotor machine is used, some differences appear between reactances along *d* and *q* axis, this is due to the inherent saliency of the machine.

For the purpose of analysing the influence of different features of the generator as: nominal power, and voltage and active power controls another synchronous machine will be used in the complex benchmark case. This second generator, also modelled by "Synchronous machine pu fundamental" *Matlab/Simulink* block, has the following characteristics:

- 15 *kV*, 200 *MVA* Round rotor machine with two pairs of poles.
- Two damper windings, one in the *d* axis and another in the *q* one.

- No Voltage Control.
- No Active Power control.

Most important parameters about transient behaviour can be seen in Table 3.2, which were obtained from [1].

$X_d$	$X_d'$	$X_d''$	$X_q$	$X_q'$	$X_q''$	$X_l$	$T_d'$	$T_d''$	$T_q'$	$T_q''$
1.65	0.23	0.17	1.59	0.38	0.17	0.1	0.83	0.023	0.42	0.023

Table 3.2: Secondary Generator Parameters

### 3.1.2 Transformers, lines and grids

#### Transformers

Two different kind of transformers are used in this thesis, all modelled by the "Three-phase transformer (two windings)" *Matlab/Simulink* block.:

- Transformer connecting the synchronous generators to the grid: as mentioned above, synchronous generators have a nominal voltage  $V_{n,generator} = 15 \text{ kV}$  and the AC grid here studied works at  $V_{n,grid} = 220 \text{ kV}$ . Therefore, one transformer is needed for the connection of each synchronous generator (one in the simple benchmark and two in the complex case). These transformer have the following features:
  - $Yg \ Yg$  connection.
  - $rt = 15/220 \text{ kV}$ .
  - $S_n = 600 \text{ MVA}$  for the transformer connecting the main generator and  $S_n = 200 \text{ MVA}$  for the secondary one.
  - $u_{cc} = 0.16 \text{ pu}$
- Transformer connecting the DC/AC converter to the grid: HVDC links usually works with a higher voltage than  $220 \text{ kV}$ , for this reason and for the purpose of adding the inductance needed for the connection of two voltage sources (as explained in Section 1.3) one transformer is used. Next characteristics define it:
  - $Yg \ Yg$  connection.
  - $rt = 370/220 \text{ kV}$
  - $S_n = 600 \text{ MVA}$
  - $u_{cc} = 0.1 \text{ pu}$

## Lines

Overhead 220 *kV* lines are used for the purpose of connecting the synchronous generators to the converter and from it to the different electrical grids. These lines are:

- Single line connecting each synchronous generator to the converter bus.
- Double line connecting the converter bus to the electrical grids (one in the simple benchmark and two in the complex case)

Most important parameters of the lines are obtained from [1], for all of them:

- $X_{line} = 0.488 \Omega/km$
- $R_{line} = 0.05 \Omega/km$

Their length is a parameter that will be modified for the different cases studied so it is not specified here.

## Grids

"Three phase sources" *Matlab/Simulink* blocks are placed in the model simulating electrical grids connected to the converter bus through overhead lines aforementioned. Most important parameters are:

- Main Grid: present in all the models
  - 220 *kV* Voltage source
  - $S_{sc} = 3 \text{ GVA}$
  - $X_{grid} = 10R_{grid}$
- Secondary Grid: only present in the complex benchmark
  - 220 *kV* Voltage source
  - $S_{sc} = 1.5 \text{ GVA}$
  - $X_{grid} = 10R_{grid}$

### 3.1.3 Converter

Modelling the converter is the key part of this work. In this section, the way to inject active and reactive power into the system will be explained, assuming that  $P$  and  $Q$  are known. Next section will be dedicated to understand how these values are obtained for the different controls proposed.

Converters can be modelled in different manners according to the purpose of the research. For transient stability studies in the case of large voltage deviations, i.e. aim of this thesis, [8] states that **it is possible to represent the converter as a simplified current controller that generates the desired currents.**

It is important to note that in this work, active and reactive power injected is always considered as the one provided to the 220 kV grid, and when the voltage control is applied, as it will be explained later on, is also done to manage this variable. However, as mentioned above (Section 3.1.2), a 370/220 kV transformer is placed between the converter and the grid, what is relevant when calculations are made.

Therefore, based on the voltage at the 220 kV bus where the converter is connected and on the reference  $P, Q$  values, needed current for each phase is calculated and injected through "Three-phase controlled current sources" blocks in *Matlab/Simulink*. In order to do so, the next strategy is followed:

First of all, phase to neutral voltages from the 220 kV bus where the converter is connected are introduced in a "PLL" block,  $\angle \overrightarrow{V_{ph-n}}$  is obtained.  $d, q$  frame is going to be used ( $q$  leading 90° with respect to  $d$ ), referenced to  $\overrightarrow{V_{ph-n}}$ . Clarke transformation which conserves the magnitude is used (it is not shown for the conciseness of the document). Therefore:

$$|\overrightarrow{V_{ph-n}}| = V_{d,ph-n} \quad (3.1)$$

$$V_{q,ph-n} = 0 \quad (3.2)$$

From now on,  $\overrightarrow{V_{ph-n}}$  will be just referred as  $\overrightarrow{V}$ .

If  $pu$  base system is used:

$$P = V_d \cdot I_d + V_q \cdot I_q \quad (3.3)$$

$$Q = V_q \cdot I_d - V_d \cdot I_q \quad (3.4)$$

According to eq. 3.2. It remains:

$$I_d = \frac{P}{V_d} \quad (3.5)$$

$$I_q = -\frac{Q}{V_d} \quad (3.6)$$

Once  $d$  and  $q$  components of the current are obtained, real  $a, b, c$  values are necessary. Firstly, Clarke Antitransformation is applied, using  $\angle \vec{V}$  coming from the "PLL" block. As the connection of the transformer between the converter and the grid is  $YgYg$  (Section 3.1.2) there is no phase shift between currents flowing through the primary (converter) and the secondary (grid) sides and this angle is the right value for this purpose. After that, as "Current controlled source" block works with real values, it is necessary to change the base frame. For each phase:

$$I_{real} = I_{pu} \frac{\sqrt{2}S_{base}}{\sqrt{3}V_{ph-ph,base}} \quad (3.7)$$

Where:

- $S_{base}$  represents the power base chosen for the converter.
- $V_{ph-ph,base}$  represents the phase to phase voltage base at the point where the current is injected. Recall that this is a 370 kV bus.
- $\sqrt{2}$  is placed because peak values and not rms ones are needed.

All this explanation gives place to the following structure in *Matlab/Simulink*, where the central block represent the  $I_d$  and  $I_q$  calculations based upon 3.5 and 3.6.

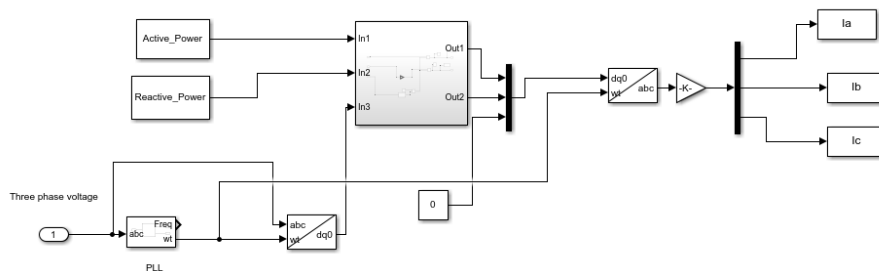


Figure 3.1: Control Scheme of the converter

## 3.2 Power Controls

Previous section was dedicated to explain how to obtain the desired active and reactive power values, supposing that they were known. In this part, these reference values will be computed depending on the kind of control that is being carried out in the converter.

Before going further it is proper to size and define the different constraints and parameters used in the converter.

- Base used for the calculations:

- $V_{base} = \frac{220}{\sqrt{3}} \text{ kV}$ .

- $S_{base} = 600 \text{ MVA}$ .

- $V_{min1} = 0.85 \text{ pu}$  and  $V_{max1} = 1.1 \text{ pu}$ , which limit the normal operation conditions.
- $V_{min2} = 0.6 \text{ pu}$  and  $V_{max2} = 1.4 \text{ pu}$  which limit the increase in reactive current during a fault.
- **Maximum power capability of the DC link is 360 MW (0.6 pu).**
- **Maximum reactive power transmission during normal operation conditions is 175 MVar (0.292 pu).** Based upon the grid codes, minimum reactive power that the converter shall be capable of provide is  $Q_{min} = 0.3 \cdot P_{max}$  (Figure 2.1). However, for this case, a possible power factor of  $\cos \varphi = 0.9$  has been set, what leads to this maximum reactive power value.
- **Maximum three-phase current** that the converter can withstand **for a short period of time** (during a fault) is  $I_{max,peak} = 1260 \text{ A}$  (0.94584 pu). Based on the values for  $P_{max}$  and  $Q_{max}$  and knowing that this injection must be possible in the range  $0.85 \leq V \leq 1.1 \text{ pu}$ ,  $I_{max,normal} = 1050 \text{ A}$ . However, physical construction of the converter allows this limit to be exceeded in a 20% during short periods.

### 3.2.1 Reactive Power in normal operation

When the grid voltage where the converter is connected is between the minimum limits ( $0.85 \leq V \leq 1.1 \text{ pu}$ ) two possible controls appear, according to what was specified in the grid codes.

### Voltage Control Mode

This control mode tries to keep the grid voltage equal to the reference specified by the grid operator. Most common controls for this purpose are composed just by a Proportional controller, however, here a small additional integral action will be set to show how this can be implemented.

Actual voltage is compared to the reference one. In this thesis a value  $V_{ref} = 1 pu$  will be always considered. Difference between them is introduced in the PI controller.

$$Q = (V_{ref} - V) \cdot (Prop + Int) \quad (3.8)$$

Where:

- $Prop$  is the proportional part. It is always set to  $Prop = 1.5$ .
- $Int$  is the integral part. During normal operation conditions it is set to  $Int = 0.1$ , however, if a fault occurs it would create a wind-up effect. Therefore, as a solution to avoid this undesirable phenomenon, its action is stopped ( $Int = 0$ ) if the voltage goes above the minimum limits.

As aforementioned, maximum reactive power injected during these conditions is  $Q_{max} = 0.292 pu$ . Therefore a saturation block is introduced.

A representation of this is shown in Figure 3.2. Matlab function implements the anti-wind up system. When the voltage is above the minimum limits, integral action is cancelled.

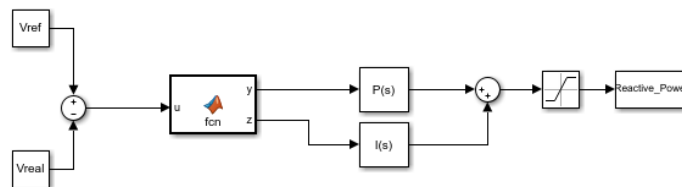


Figure 3.2: Scheme of voltage control mode

### Reactive Power Control mode

This mode is based on following the reference specified by the grid operator for the reactive power. Hence, there is nothing to do in order to calculate this value.

### 3.2.2 Active Power in normal operation

Depending on the capability for carrying out frequency control, two models will be developed :

#### Frequency Sensitive mode

In addition to the reference active power specified by the grid operator, some extra power will be injected according to the deviation of the frequency with respect to the nominal value (50 Hz). As specified in the grid codes, this action must occur when the frequency goes above a certain deadband and shall be proportional to its deviation through a constant droop term.

$$P_{total} = P_{reference} + P_{frequency} \quad (3.9)$$

$$P_{frequency} = -\sigma \cdot (f - f_n) \quad (3.10)$$

Where:

- $P_{frequency} = 0$  if  $49.8 \leq f \leq 50.2$  Hz, representing the deadband.
- $\sigma$  represents the droop term,  $\sigma = 5\% \cdot P_{max}/Hz$ .
- Overfrequency situations are associated to an excess of active power in the system, therefore it is necessary to reduce this power injection to recover the reference value. Otherwise, if frequency decreases beyond the limits, more power is needed in the system. This explanation justifies the negative sign present in the equation.

In accordance to the converter constraints explained above, a saturation block is introduced to limit the power injection to  $P = 0.6 pu$ .

#### Non Frequency sensitive mode

One model where the system is not able to react against frequency deviations is developed in order to check the effect of the Frequency sensitive one. In this case, active power injection is always equal to the reference value specified by the grid operator. Over and Underfrequency sensitive modes are not developed for the sake of conciseness because for the study of these kind of faults they would not exhibit much differences from the two ones developed.

$$P = P_{Reference} \quad (3.11)$$

### 3.2.3 Control during fault situation

As this thesis is based on the study of large disturbances, specific actions to be done in the converter when such a problem occurs are crucial. Recall that these situations are considered when:

$$V > 1.1 \text{ pu} \quad \text{or} \quad V < 0.85 \text{ pu} \quad (3.12)$$

Three possible controls are here presented:

#### Give priority to the reactive power

As specified in the Spanish and Belgian grid codes, in the case of large disturbances, extra reactive power should be injected in addition to the one coming from the "normal operation control".

$$Q_{total} = Q_{normal} + Q_{extra} \quad (3.13)$$

This extra power is calculated based on the maximum current that the converter can withstand in accordance to Figure 2.4.

For the case of undervoltage situation:

$$Q_{extra} = V \cdot \frac{I_{max} - Q_{normal}/V}{V_{min1} - V_{min2}} \cdot (V_{min1} - V) \quad (3.14)$$

For the case of overvoltage situation:

$$Q_{extra} = V \cdot \frac{-I_{max} - Q_{normal}/V}{V_{max2} - V_{max1}} \cdot (V - V_{max1}) \quad (3.15)$$

Where:

- $V_{min1} = 0.85 \text{ pu}$  and  $V_{min2} = 0.6 \text{ pu}$
- $V_{max1} = 1.1 \text{ pu}$  and  $V_{max2} = 1.4 \text{ pu}$
- $I_{max} = 0.94584 \text{ pu}$

Obviously, these results are limited to the maximum current value.

If  $V_{min2} \leq V \leq V_{min1}$  and  $V_{max1} \leq V \leq V_{max2}$  it can be noticed that  $I < I_{max}$ . If this occurs, active power shall be provided until the current limitation is reached.

Therefore:

$$P = V \cdot \sqrt{I_{max}^2 - (Q/V)^2} \quad (3.16)$$

Otherwise, if voltage is above the maximum limits:

$$P = 0 \quad (3.17)$$

This strategy is roughly shown in Figure 3.3 where the function blocks introduce the equations aforementioned and  $Q_{normal}$  and  $P_{normal}$  values come from the control modes for the normal operation conditions.

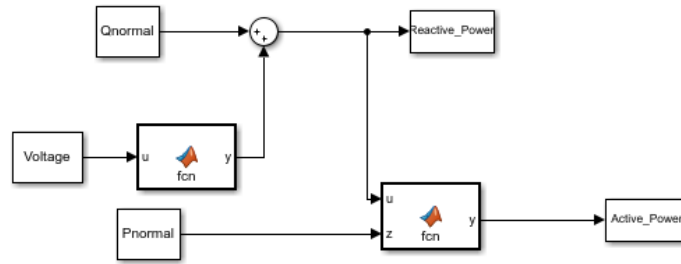


Figure 3.3: Scheme of prior reactive power control mode

### Give priority to the active power

In the European grid codes it is not specified the control to be done in the case of a large disturbance. Therefore, it is going to be compared with a model where the active power injection is imperative.

In a similar way to the procedure for the case where the reactive power was imperative:

$$P_{total} = P_{normal} + P_{extra} \quad (3.18)$$

For an undervoltage situation:

$$P_{extra} = V \cdot \frac{I_{max} - P_{normal}/V}{V_{min1} - V_{min2}} \cdot (V_{min1} - V) \quad (3.19)$$

For the case of an overvoltage situation:

$$P_{extra} = V \cdot \frac{I_{max} - P_{normal}/V}{V_{max2} - V_{max1}} \cdot (V - V_{max1}) \quad (3.20)$$

However, as it can be seen, in this case it is always considered as a power injection. It is due to several reasons:

- In this work, both HVDC links and Power park modules are being treated. Therefore, in the later case, big power consumptions are not possible as it would lead to major problems.
- During large disturbances many loads cannot be energized, therefore, with this power injection some loads closed to the converter could remain connected during the fault.
- It could lead to major problems if the power demanded by the converter cannot be provided by the system. Indeed, during simulations, if power demanded during the fault was high enough solver could not reach a solution and this seem to be the explanation.

Again, if  $I < I_{max}$  reactive power shall be injected in order to reach this value.

For an undervoltage situation:

$$Q = V \cdot \sqrt{I_{max}^2 - (P/V)^2} \quad (3.21)$$

For the case of an overvoltage situation:

$$Q = -V \cdot \sqrt{I_{max}^2 - (P/V)^2} \quad (3.22)$$

Otherwise, if voltage is above the maximum limits:

$$Q = 0 \quad (3.23)$$

This strategy is roughly shown in Figure 3.4 where the function blocks introduce the equations aforementioned and  $Q_{normal}$  and  $P_{normal}$  values come from the control modes for the normal operation conditions.

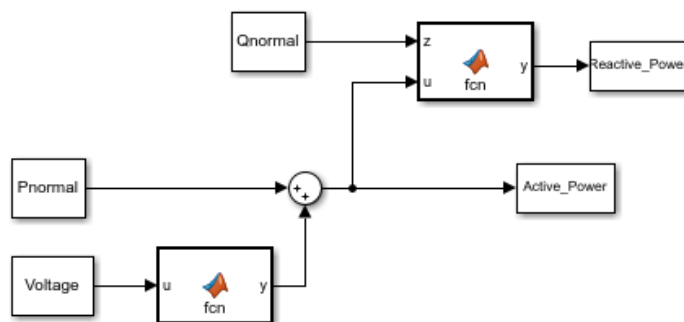


Figure 3.4: Scheme of prior active power control mode

### No Control at all

In order to compare the other two actions, a model where neither active nor reactive power is injected during the fault.

$$P = 0 \quad Q = 0 \tag{3.24}$$

All these strategies seem to have been developed uniquely for the case of a symmetrical fault. However, in this thesis, single line to ground faults are also analysed. In accordance to [9], for synchronous machine stability purposes, i.e. the aim of these thesis, no negative sequence current injection is the best option. Therefore, **these models are also valid for the study of this kind of asymmetrical disturbances**. But note that, in this case, **the control will be done in the direct voltage sequence component ( $V_1$ ) and not in the global value**.

### 3.2.4 Grid Configuration

Finally, all these controls are going to be implemented in two different grid benchmarks.

#### Simple Benchmark

This model is implemented without loads and with only one grid connected to the converter. Therefore, this seems to be the most critical situation for the transient stability of the machine.

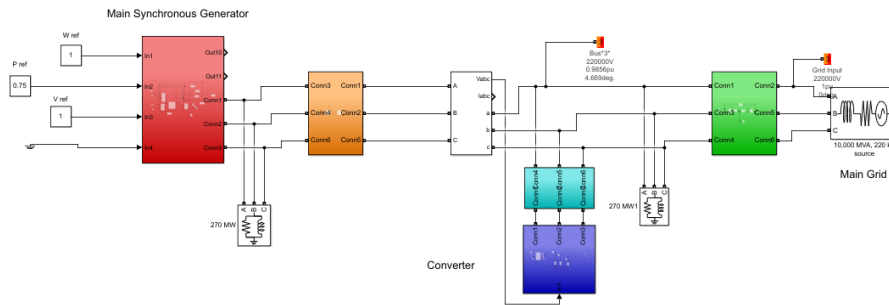


Figure 3.5: Simple Benchmark

In Figure 3.5 a scheme of the benchmark used for this purpose is presented. Red block represents the synchronous generator, connected to a transformer (orange block). Blue blocks are the converter and the transformer which connects it to the grid. Finally, green block simulates the overhead line which connects the 3GVA grid, and where the fault occurs. In addition, two 300 MVA and  $\cos(\varphi) = 0.9$  loads are placed.

### Complex Benchmark

However, a more realistic situation is here being sought. With this purpose a "Complex" benchmark has been developed. This model, with respect to the previous one introduces:

- **Synchronous generator:** one non controlled, less powerful (200 *MVA*) machine.
- **Secondary grid:** in parallel with the main one,  $S_{sc} = 1.5 \text{ GVA}$
- **Line connecting generators to the converter bus:** overhead line with same parameters as the ones explained in the previous section ( $R = 0.05\Omega/km$   $X = 0.488\Omega/km$ )
- **Loads** connected at different points of the grid:
  - 100 *MVA* and  $\cos(\varphi) = 0.9$  connected in parallel to the secondary synchronous generator.

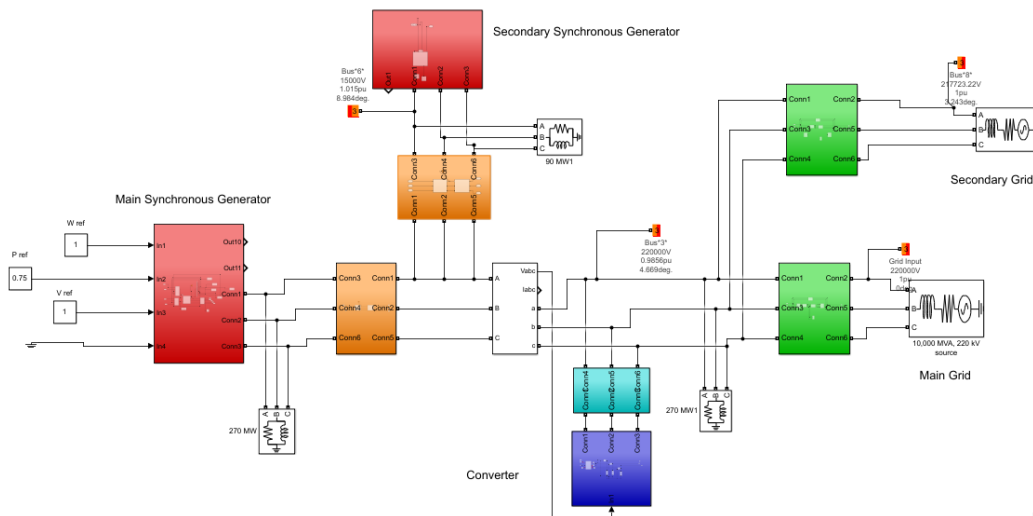


Figure 3.6: Complex Benchmark

# Chapter 4

## Results

It is now time to show the different results that have arisen from the application, to different situations, of the control modes and benchmarks previously presented.

In this chapter, voltage dips at the converter and at the synchronous generator buses during the fault will be shown, as well as their transient behaviour until they reach a new steady state. In the next chapter, influence of this situation on the different variables of the synchronous generator will be analysed.

These results will be studied for different cases, in order to check separately the influence of the normal operation conditions control modes (cases 1 and 2) and the "fault" ones (cases 1,3 and 4). **It is really important to notice that along the document all these 4 control models developed will be named in this way (Case 1, Case 2, Case 3 and Case 4):**

- **Case 1**
  - Reactive Power control in normal operation conditions: **Voltage control mode**
  - Active Power control in normal operation conditions: **Frequency sensitive mode**
  - Control during the fault: **Reactive Power priority**
- **Case 2**
  - Reactive Power control in normal operation conditions: **Reference reactive power control mode**

- Active Power control in normal operation conditions: **Frequency sensitive mode**
- Control during the fault: **Reactive Power priority**
- **Case 3**
  - Reactive Power control in normal operation conditions: **Voltage control mode**
  - Active Power control in normal operation conditions: **Frequency sensitive mode**
  - Control Power during the fault: **Active Power priority**
- **Case 4**
  - Reactive Power control in normal operation conditions: **Voltage control mode**
  - Active Power control in normal operation conditions: **Frequency sensitive mode**
  - Control during the fault: **No Control at all**

For the reactive power analysis, Voltage and Reference reactive Power control modes behave, as it will be seen, in a really similar way during the fault period, and they only exhibit differences during the post-fault situation. Therefore, for the sake of conciseness only one of this modes (Voltage control) will be set for the study of the control action during the fault (cases 3 and 4).

In addition, as it will also be shown in Figure 4.5, frequency deviation is really low, therefore, there is nearby no difference between frequency and non frequency sensitive modes. Hence, again for the sake of conciseness, only the frequency sensitive mode will be used for all the cases studied.

For all the simulations carried out, following setpoints have been fixed  $S_b = 600 MW$ :

- Active power injection of Synchronous generator 1= 450 MW(0.75 pu)
- Active power injection of Synchronous generator 2= 180 MW(0.3 pu)
- Reference active power injection for the converter= 330 MW(0.55 pu)

In addition, important extra parameters to recall are:

- Length of double line connecting the converter and the main grid = 75 km
- Length of double line connecting the converter and the secondary grid = 40 km
- Length of single line connecting the converter and the synchronous generator (main and secondary) = 5 km (Although it will be changed in some situations for influence analysis purposes).
- Maximum Current allowed by the converter = 0.94584 pu (Although it will be changed in some situations for influence analysis purposes).

Regarding the disturbance occurring at the system:

- It will occur at some point (variant for different influence analysis purposes) of one of the two lines connecting the main grid and the converter.
- Fault is cleared after 150ms by the disconnection of the faulty line so the connection between converter and main grid becomes a single line one.
- Three-phase fault is also connected to the ground.
- Single line ground fault occurs on phase A.

Once all the different cases (control models developed) have been presented. This analysis is going to be carried out regarding three completely different situations:

- **Three-phase fault in the Complex benchmark:** for the purpose of studying the influence of different parameters of the system,
  - Distance from the converter to the fault (for a constant distance of 5 km from the synchronous generators to the converter and  $I_{max} = 0.94584 pu$ ):
    - \* 12.5 km
    - \* 25 km
    - \* 37.5 km
    - \* 50 km
  - Distance from the synchronous generator to the converter (for a constant distance of 25 km from the converter to the fault and  $I_{max} = 0.94584 pu$ ):
    - \* 5 km
    - \* 10 km
    - \* 15 km
    - \* 20 km

- Maximum current allowed (for a constant distance of 5 *km* from the synchronous generators to the converter and of 25 *km* from the converter to the fault):
  - \*  $1.1 \cdot I_{max} = 1.1 \cdot 0.94584 \text{ pu}$
  - \*  $1.2 \cdot I_{max} = 1.2 \cdot 0.94584 \text{ pu}$
  - \*  $1.3 \cdot I_{max} = 1.3 \cdot 0.94584 \text{ pu}$
- **SLG fault in the Complex benchmark:** all four cases (models developed) will be compared for the complex benchmark configuration with 25 *km* distance from the converter to the fault, 5 *km* distance from the synchronous generator to the converter and a maximum allowed current  $I_{max} = 0.94584 \text{ pu}$ .
- **Three-phase fault in the Simple benchmark:** all four cases (models developed) will be computed for the simple benchmark case with 25 *km* distance from the converter to the fault and for a maximum allowed current  $I_{max} = 0.94584 \text{ pu}$ .

## 4.1 Theoretical approach

For the purpose of ensuring the validity of the results a theoretical estimation will be provided. It is applied to the Complex Benchmark as the effectiveness for this case would guarantee the Simple benchmark ones. Moreover, for the sake of simplicity, three-phase shortcircuit fault will be studied, so just the direct sequence circuit will be represented.

This estimation is based on comparing the voltage during the fault in function of the power injected by the converter in this period. According to [10], a valid estimation for the voltage dip along two points  $V_1$  and  $V_2$  is:

$$\Delta V = V_1 - V_2 \approx \frac{RP + QX}{V_1} \quad (4.1)$$

Which can be expressed as:

$$\Delta V = V_1 - V_2 \approx RI_d - I_qX \quad (4.2)$$

Where:

- $X$  and  $R$  are the impedance values between those two points.
- $P$  and  $Q$  are the power values going from point 1 to point 2.
- $I_d$  and  $I_q$  are the  $d, q$  components of the current flowing from point 1 to point 2 referred to the  $V_1$  phasor.

Kind of Superposition principle is applied. The system is decomposed into two subsystems (Figure 4.1 and Figure 4.2) first of them composed of the different electrical sources in the system (synchronous generators and electrical grids). Action of the converter during the fault is presented in subsystem two (Figure 4.2). It is really important to add some other sources apart from the converter in order to provide the additional current that is needed in Subsystem 2, as grid is composed by different resistances and reactances it is not possible to inject only active (resp. reactive) current (which will induce reactive (active) losses in the reactances (resistances)) without injecting reactive (active) power to compensate them. This power is supposed to be provided by the different sources of the system (synchronous generators and electrical grids). Red current sources in the scheme represent this effect.

$$\Delta V = V_1 - V_2 \approx R(I_{d1} + I_{d2}) - (I_{q1} + I_{q2})X \quad (4.3)$$

- $I_{d1}$  and  $I_{q1}$  being the  $d$  and  $q$  components, respectively, of the current coming from subsystem 1.
  
- $I_{d2}$  and  $I_{q2}$  being the  $d$  and  $q$  components, respectively, of the current coming from subsystem 2.

Superposition principle states that currents for the complete system are equal to the sum of currents coming from the subsystems into which it is divided. For this estimation, as  $d, q$  components are used, it is going to be supposed that the electrical angle  $\angle \vec{V}_1$  does not vary from its value in subsystem 1 to the one in the complete system. Therefore equality of currents is also truth for  $d, q$  components. This does not mean a problem for subsystem 2, as it is referred to the currents coming from the converter, which are already expressed in the  $d, q$  frame and are adapted depending on the electrical angle of  $V_1$ .

This assumption is mostly truth for the case of reactive power injection during the fault. However, for the case where active power has priority it could lead to slight deviations and, so on, to inaccuracy in the results.

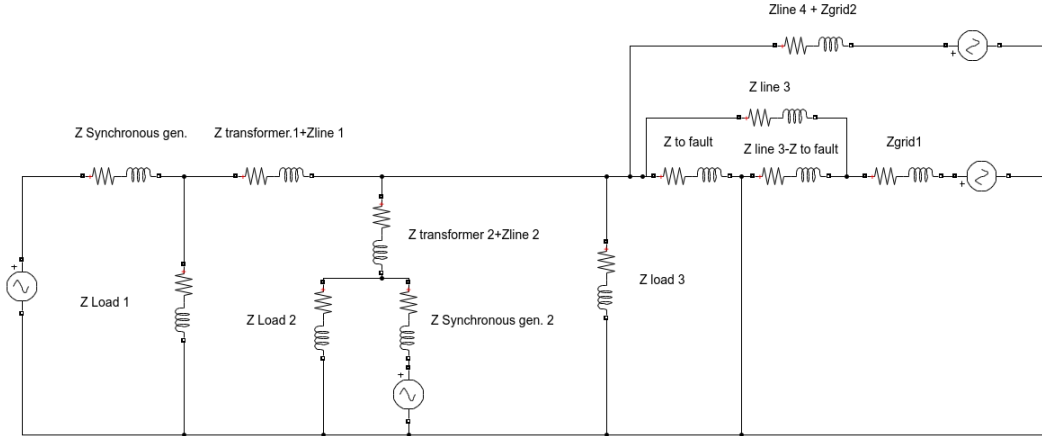


Figure 4.1: Subsystem 1

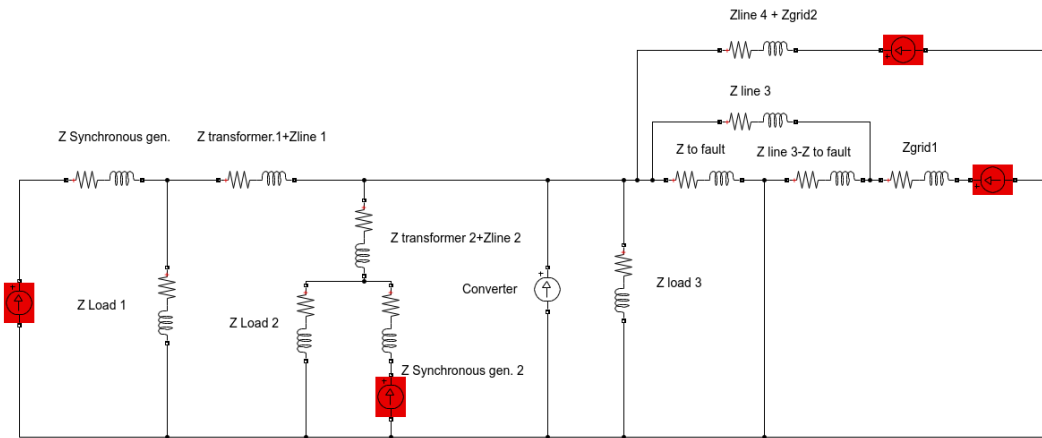


Figure 4.2: Subsystem 2

Once the subsystems are presented and main comments and assumptions are done, we have to find the theoretical effect of each control mode. It is obtained in the following way:

Non-controlled system (Case 4) does not inject any power during the fault ( $P = 0$  and  $Q = 0$ ). Therefore, subsystem 2 (Figure 4.2) would not have any consequence on the system. Otherwise, if power is injected based on the different controls proposed (Cases 1,2 and 3), subsystem 2 would create different voltages dips along the line.

$$\Delta V_{total} = \Delta V_{subsystem1} + \Delta V_{subsystem2} \quad (4.4)$$

- $\Delta V_{subsystem1}$  being the  $\Delta V$  due to currents from subsystem 1.
- $\Delta V_{subsystem2}$  being the  $\Delta V$  due to currents from subsystem 2.

If no power is injected during the disturbance

$$\Delta V_{noncontrolled,subsystem2} = 0 \quad (4.5)$$

Otherwise, when power is injected:

$$\Delta V_{controlled,subsystem2} \neq 0 \quad (4.6)$$

Hence, supposing that  $\Delta V_{subsystem1}$  is equal for both controlled and non controlled systems, effect of each controller in the voltage, named as  $\Delta V_{effect}$ , can be computed.

$$\Delta V_{effect} = \Delta V_{controlled,subsystem2} \quad (4.7)$$

Values for the different impedances are (in p.u.  $S_b = 600 \text{ MVA}$   $V_b = 220/\sqrt{3}$ ):

- $Z_{sync.gen.1} = 2.854 \cdot 10^{-3} + j0.39 \text{ pu}$
- $Z_{synch.gen.1} = 8.562 \cdot 10^{-3} + j0.69 \text{ pu}$
- $Z_{transf.1} = j0.16 \text{ pu}$
- $Z_{transf.2} = j0.48 \text{ pu}$
- $Z_{line.1} = Z_{line.2} = Dist_{conv,synch} \cdot (6.198 \cdot 10^{-4} + j6.050 \cdot 10^{-3})$
- $Z_{load.1} = Z_{load.3} = 2.22 + j4.59 \text{ pu}$
- $Z_{load.2} = 6.66 + j13.765 \text{ pu}$
- $Z_{toFault} = Dist_{Conv_{fault}} \cdot (6.198 \cdot 10^{-4} + j6.050 \cdot 10^{-3})$
- $Z_{line3} = 0.046485 + j0.45375 \text{ pu}$
- $Z_{line4} = 0.0124 + j0.121 \text{ pu}$
- $Z_{grid1} = 0.0199 + j0.199 \text{ pu}$
- $Z_{grid2} = 0.0398 + j0.398 \text{ pu}$

Two considerations are taken while defining the reactances representing the synchronous machine  $X_{sync.gen.1}$  and  $X_{sync.gen.2}$ : both machines, as specified previously, are round rotor ones, however, there is a slight difference in  $d$  and  $q$  reactances. For the sake of simplicity, average value between the two terms is used. In addition, as during the fault reactances values are changing, it is necessary to choose one. Subtransient reactances are used for this purpose, so  $\Delta V$  values occurring at the beginning of the fault are the ones which must be measured.

Impedances above shown are clearly dependent on the parameters that are going to be varied on the system, namely :distance from the converter to the fault and distance from the synchronous generator to the converter. Moreover,  $P$  and  $Q$  are dependent on the maximum current allowed by the converter ( $I_{max}$ ).

$\Delta V_{effect}$  will be computed for the 15 kV and 220 kV buses, as they are the most important ones, and for all the possibilities studied regarding the distance from the converter to the fault (Table 4.1), distance from the converter to the synchronous generator (Table 4.2) and maximum current allowed by the converter (Table 4.3). As it can be noticed, this effect only depends on the action taken during the fault, hence, Active and Reactive power priority are analyzed independently of the control done during "normal operation conditions" (Case1=Case2 for the reactive power priority and Case 3 for the active one).

For calculating  $\Delta V_{effect,220\text{ kV}}$  the equivalent impedance seen from the converter will be obtained. Based on this value and on the impedance connecting 15 kV and 220 kV buses  $\Delta V_{effect,15\text{ kV}}$  is deduced.

For the active power case it will be considered that only active current is flowing into the system and therefore the voltage drop is computed only on the resistances:

$$\Delta V_{effect,220\text{ kV}} = I_p \cdot R_{total} \quad (4.8)$$

$$\Delta V_{effect,15\text{ kV}} = \Delta V_{effect,220\text{ kV}} - \frac{\Delta V_{effect,220\text{ kV}}}{R_1} \cdot R_2 \quad (4.9)$$

Where, for all the situations  $I_p = I_{max}$ .

For the reactive power case it will be considered the opposite situation, only reactive current flowing into the system and therefore voltage drop computed on the reactances :

$$\Delta V_{effect,220\text{ kV}} = -I_q \cdot X_{total} \quad (4.10)$$

$$\Delta V_{effect,15\text{ kV}} = \Delta V_{effect,220\text{ kV}} - \frac{\Delta V_{effect,220\text{ kV}}}{X_1} \cdot X_2 \quad (4.11)$$

Where, for all the situations  $I_q = I_{max}$ .

$R_1$  and  $X_1$  are the resistances and reactances, respectively, connecting the converter to the ground through the 15 kV bus path, and  $R_2$  and  $X_2$  are the ones connecting the converter and the 15 kV bus.

		12.5 km	25 km	37.5 km	50 km
Active Power priority	$\Delta V_{220}$ (pu)	0.0045	0.0064	0.0074	0.0080
	$\Delta V_{15}$ (pu)	0.0026	0.0038	0.0044	0.0048
Reactive Power priority	$\Delta V_{220}$ (pu)	0.0469	0.0695	0.0827	0.0909
	$\Delta V_{15}$ (pu)	0.0277	0.0411	0.0489	0.0538

Table 4.1: Theoretical approach.Distance to fault influence

		5 km	10 km	15 km	20 km
Active Power priority	$\Delta V_{220}$ (pu)	0.0064	0.0066	0.0067	0.0069
	$\Delta V_{15}$ (pu)	0.0038	0.0036	0.0035	0.0034
Reactive Power priority	$\Delta V_{220}$ (pu)	0.0695	0.0704	0.0711	0.0718
	$\Delta V_{15}$ (pu)	0.0411	0.0391	0.0372	0.0355

Table 4.2: Theoretical approach. Distance to synchronous generator influence

		Imax	Imax*1.1	Imax*1.2	Imax*1.3
Active Power priority	$\Delta V_{220}$ (pu)	0.0064	0.0070	0.0077	0.0083
	$\Delta V_{15}$ (pu)	0.0038	0.0042	0.0045	0.0049
Reactive Power priority	$\Delta V_{220}$ (pu)	0.0695	0.0765	0.0834	0.0904
	$\Delta V_{15}$ (pu)	0.0411	0.0452	0.0494	0.0535

Table 4.3: Theoretical approach. Maximum allowed current by the converter influence

## 4.2 Experimental Results

In Section 4.2.1, results of the three-phase fault case will be shown, SLG ones in Section 4.2.2 and finally, three-phase fault in the Simple benchmark in Section 4.2.3. In each part, numerical results are shown in Tables and, for a better understanding of the vaules, some

of them are plot. Finally, at the end, proper comments for each case are made.

### 4.2.1 Three-phase fault

For the purpose of comparing both fault and postfault behaviour of the different controls.  $V_{15}$  and  $V_{220}$  during the fault,  $V_{15,peak}$  once the fault is cleared and time  $t_{stab}$  representing the time it needs to reach  $\pm 1\%$  of the final value will be obtained. These post-fault vaules are chosen for the 15 kV bus as it is where the generator is connected and therefore, they are more important for analysing the effect on the machine.

#### Distance to fault influence

In Table 4.4 main results can be observed for the case of variant distance to fault and 5 km to generator and  $I_{max} = 0.94584pu$ . In order to compare the controls, their effect on the 15 kV bus is shown in 4.3 for the specific situation of 25 km to fault. Figure 4.4 plots the effect of the distance to fault on one specific case (Case 1). Finally, Figure 4.5 shows the frequency at the connection point of the converter, as it is noticed, it only deviates slightly and for a short period above the deadband ( $49.8 \leq f \leq 50.2Hz$ ) what demonstrates that the frequency sensitive mode does not influence a lot in the system.

		12.5 km	25 km	37.5 km	50 km
Case 1	$V_{220}$ (pu)	0.35	0.5145	0.607	0.6476
	$V_{15}$ (pu)	0.61	0.708	0.7646	0.7926
	$V_{15,peak}$ (pu)	1.027	1.021	1.017	1.0168
	$t_{stab}$	1.69	1.5	0.82	0.815
Case 2	$V_{220}$ (pu)	0.35	0.5145	0.6065	0.6446
	$V_{15}$ (pu)	0.61	0.708	0.7642	0.789
	$V_{15,peak}$ (pu)	1.028	1.022	1.0182	1.019
	$t_{stab}$	1.71	1.55	0.83	0.83
Case 3	$V_{220}$ (pu)	0.307	0.4505	0.5272	0.5653
	$V_{15}$ (pu)	0.586	0.6744	0.7214	0.745
	$V_{15,peak}$ (pu)	1.03	1.025	1.023	1.022
	$t_{stab}$	2.55	1.71	1.7	1.69
Case 4	$V_{220}$ (pu)	0.3037	0.4456	0.5212	0.559
	$V_{15}$ (pu)	0.5817	0.6665	0.7122	0.735
	$V_{15,peak}$	1.029	1.0245	1.0213	1.0195
	$t_{stab}$	1.71	1.67	1.59	0.83

Table 4.4: Experimental  $V_{15}$  and  $V_{220}$ . Distance to fault influence.

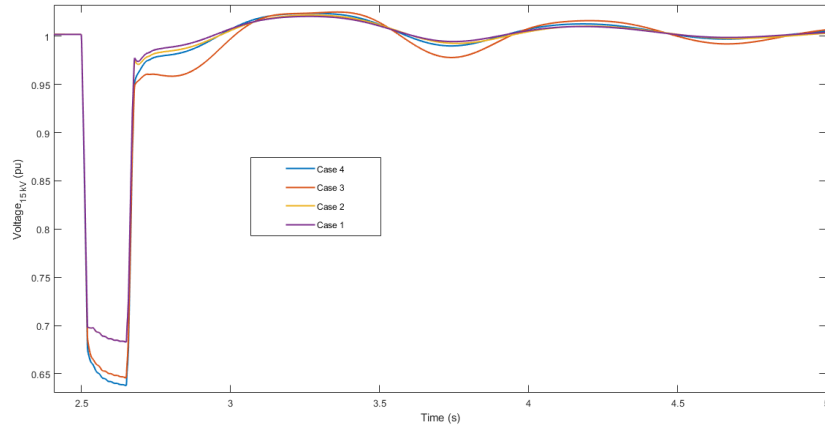


Figure 4.3: Control Comparison, 25 km to fault, 5 km to generator and  $I_{max} = 0.94584$

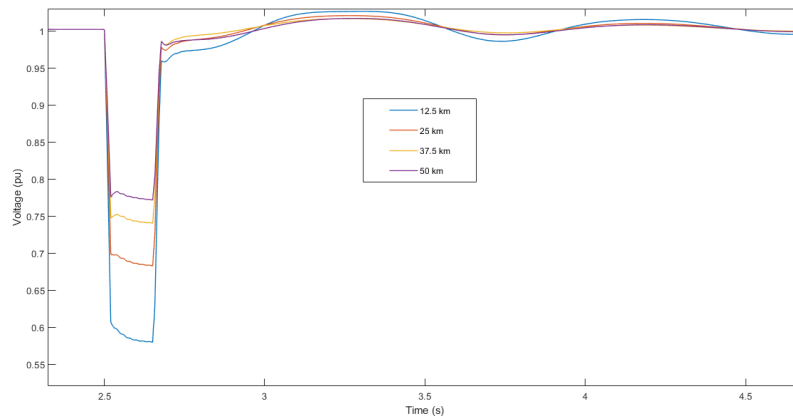


Figure 4.4: Case 1, Distance to fault influence

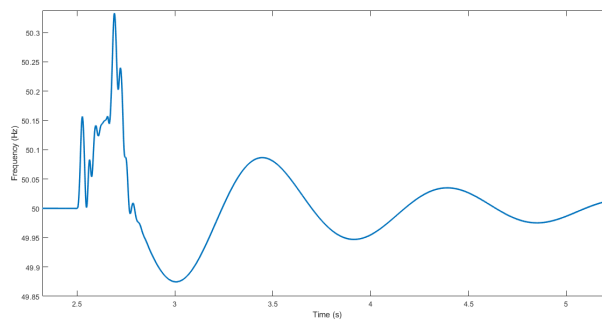


Figure 4.5: Frequency of the grid at the connection point of the converter

**Maximum allowed current influence**

In Table 4.5 main results can be observed for the case of maximum current allowed.

		Imax	Imax*1.1	Imax*1.2	Imax*1.3
Case 1	$V_{220}$ (pu)	0.5145	0.5213	0.5281	0.535
	$V_{15}$ (pu)	0.708	0.7124	0.71655	0.72065
	$V_{15,peak}$ (pu)	1.021	1.0208	1.0205	1.0205
	$t_{stab}$	1.5	1.45	0.85	0.85
Case 2	$V_{220}$ (pu)	0.5145	0.5213	0.5281	0.535
	$V_{15}$ (pu)	0.708	0.7124	0.71655	0.72065
	$V_{15,peak}$ (pu)	1.022	1.0225	1.0215	1.0212
	$t_{stab}$	1.55	1.59	1.48	0.85
Case 3	$V_{220}$ (pu)	0.4505	0.4504	0.4503	0.4500
	$V_{15}$ (pu)	0.6744	0.6746	0.6747	0.6748
	$V_{15,peak}$ (pu)	1.025	1.026	1.026	1.0255
	$t_{stab}$	1.71	1.73	1.73	1.69
Case 4	$V_{220}$ (pu)	0.4456	0.4456	0.4456	0.4456
	$V_{15}$ (pu)	0.6665	0.6665	0.6665	0.6665
	$V_{15,peak}$	1.0245	1.0245	1.0245	1.0245
	$t_{stab}$	1.67	1.67	1.67	1.67

Table 4.5: Experimental  $V_{15}$  and  $V_{220}$ . Maximum Current influence. 25 km to fault and 5 km to generator

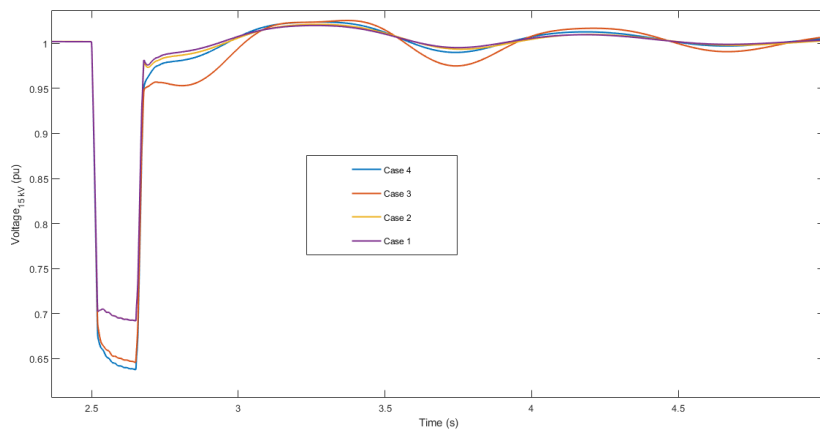


Figure 4.6: Controls comparison, 25 km to fault and 5 km to synchronous generator

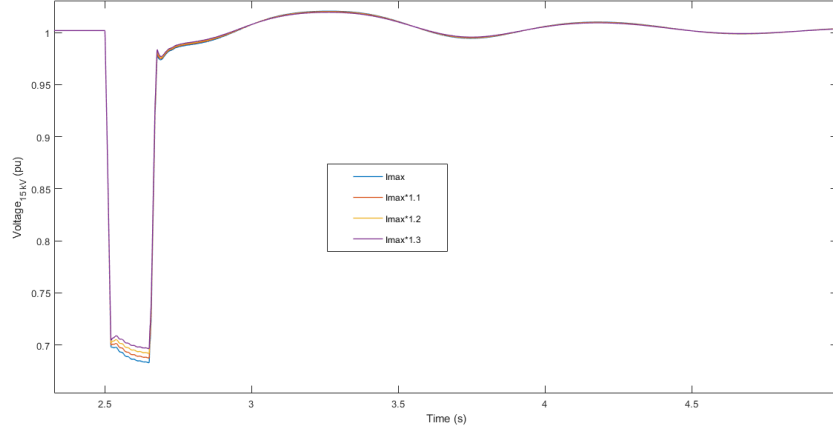


Figure 4.7: Case 1, Maximum current influence

In order to compare the controls, their effect on the 15 kV bus is shown in 4.6 for the specific situation of  $I_{max} = 1.2 * 0.94584pu$ . Finally, Figure 4.7 plots the effect of the distance to fault on one specific case (Case 1).

### Distance to Synchronous generator influence

		5 km	10 km	15 km	20 km
Case 1	$V_{220}$ (pu)	0.5145	0.5086	0.5032	0.4984
	$V_{15}$ (pu)	0.708	0.7224	0.7351	0.7466
	$V_{15,peak}$ (pu)	1.021	1.0212	1.0214	1.0216
	$t_{stab}$	1.5	1.61	1.65	1.67
Case 2	$V_{220}$ (pu)	0.5145	0.5086	0.5032	0.535
	$V_{15}$ (pu)	0.708	0.7224	0.7351	0.72065
	$V_{15,peak}$ (pu)	1.022	1.0222	1.0224	1.0225
	$t_{stab}$	1.55	1.64	1.66	1.67
Case 3	$V_{220}$ (pu)	0.4505	0.444	0.4378	0.4324
	$V_{15}$ (pu)	0.6744	0.6905	0.705	0.71835
	$V_{15,peak}$ (pu)	1.025	1.026	1.026	1.026
	$t_{stab}$	1.71	1.73	1.79	1.83
Case 4	$V_{220}$ (pu)	0.4456	0.4389	0.4329	0.4275
	$V_{15}$ (pu)	0.6665	0.6827	0.6973	0.7107
	$V_{15,peak}$	1.0245	1.0245	1.0246	1.0248
	$t_{stab}$	1.67	1.7	1.73	1.76

Table 4.6: Experimental  $V_{15}$  and  $V_{220}$ . Distance to generator influence

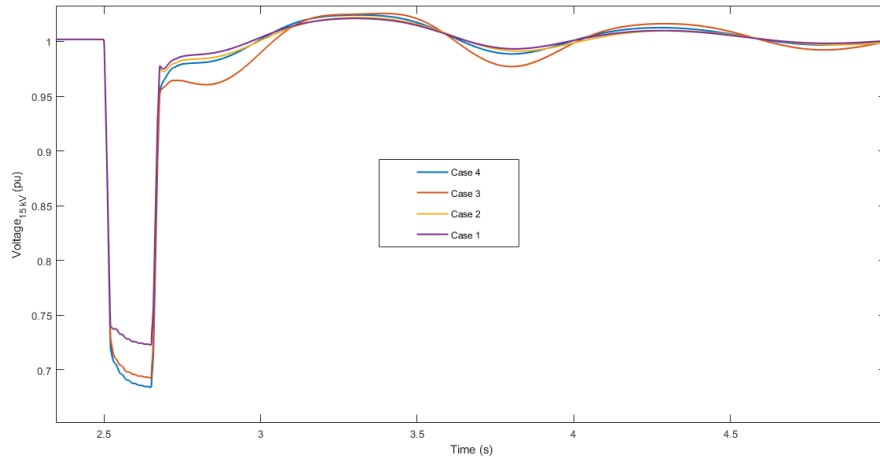


Figure 4.8: Controls comparison, Distance converter to generator influence

In Table 4.6 main results can be observed for the case of variant distance to generator with 25 km to fault and  $I_{max} = 0.94584pu$ . In order to compare the controls, their effect on the 15 kV bus is shown in Figure 4.8 for the specific situation of 5 km to generator. Comparison for just one case is not done due to the grid composition is different so conclusions coming from these visual results would not be so clear.

Three main conclusions can be derived from these results:

- Voltage and Reference Reactive power control modes do not exhibit differences. They were set in a way that reactive power injected previously to the fault was the same in both cases. Therefore, if  $V_{220} < 0.6pu$  and maximum current is injected, their behaviour during the fault is exactly equal and only slight deviations can be seen in the post fault situation and voltage controller does not seem to interact a lot with the synchronous generator one.

However, two comments can be done to this statement: firstly, if the power set by the reactive power control mode is different to the one coming from the voltage control mode, some deviations appear. As it is shown in (Figure 4.9), if reference reactive power is higher (for example 0.2 pu) than the one coming from the voltage control mode (0.02pu), in order to balance the system, power coming from synchronous machine is lower. If this occurs, and during the fault (if  $V_{220} kV < 0.6pu$ ) same current is injected through the converter, a bit lower reactive current flows into the system, and  $V_{15}$  and  $V_{220}$  decrease slightly. On the other hand, if reference reactive power is lower (for example 0.2 pu) than the one injected by the Voltage control mode previously to the fault, opposite situation takes place and  $V_{15}$  and  $V_{220}$  increase. Moreover, if powers are set to be equal in the pre-fault situation but,

during the fault,  $0.6 < V_{220 \text{ kV}} < 0.85 \text{ pu}$  different power are injected by the two control modes, as it is the sum of  $I_q$  coming from the control mode in the "normal situation conditions" plus  $\Delta I_r$  and the first will be bigger for the voltage control mode. Therefore,  $V_{15 \text{ kV}}$  and  $V_{220 \text{ kV}}$  will be slightly higher for the voltage control mode, as it can be seen in Table 4.4 specially for the  $50 \text{ km}$  distance to fault case.

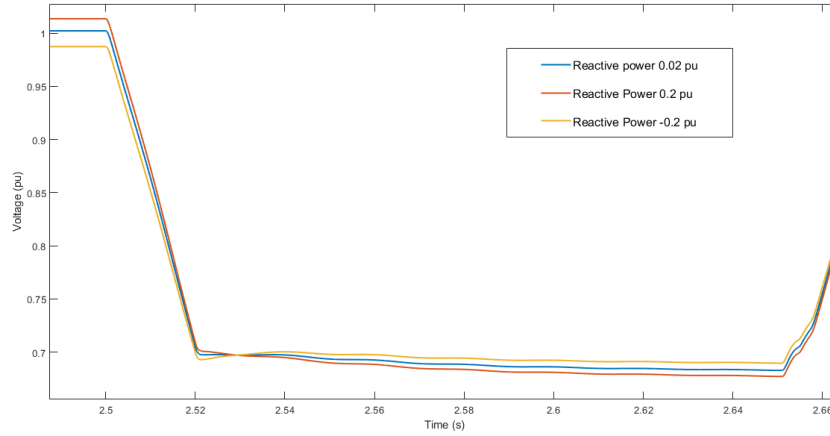


Figure 4.9: Reactive Power control comparison for different references

- Active power priority has a much lower impact than the reactive power priority case. Due to the fact that, as it is well know, reactive power is the one related to voltage drops.
- Impact of the different parameters on the fault are: increasing distance to fault means a higher effect of the controllers on the voltage, as the equivalent impedances seen by  $220 \text{ kV}$  and  $15 \text{ kV}$  buses are bigger. The higher current allowed by the converter, the higher voltage effect in both  $220 \text{ kV}$  and  $15 \text{ kV}$  buses. Referred to the distance from the generator to the converter, as the grid configuration is changed, it is better to see their influence compared to the non control case for each situation, as it is shown in 4.14 and 4.15.

#### 4.2.2 Single line ground fault

In this section, SLG fault case is analysed, in order to do so inverse and direct sequence components of the voltage at the  $15 \text{ kV}$  and  $220 \text{ kV}$  buses ( $V_{1,15}$ ,  $V_{2,15}$  and  $V_{1,220}$  and  $V_{2,220}$  respectively ) are obtained. Values for the  $15 \text{ kV}$  are shown in Figures 4.10 and 4.11. Situation studied is regarding  $12.5 \text{ km}$  distance to fault  $5 \text{ km}$  distance to synchronous generator and  $I_{max} = 0.94584 \text{ pu}$ .

	$V_{1,220}$ (pu)	$V_{2,220}$ (pu)	$V_{1,15}$ (pu)	$V_{2,15}$ (pu)	$V_{max,15}$ (pu)
Case 1	0.815	0.209	0.89	0.1245	1.175
Case 2	0.796	0.205	0.878	0.122	1.155
Case 3	0.848	0.217	0.91	0.129	1.21
Case 4	0.766	0.198	0.851	0.118	1.135

Table 4.7: Experimental  $V_{15}$  and  $V_{220}$ . SLG fault.

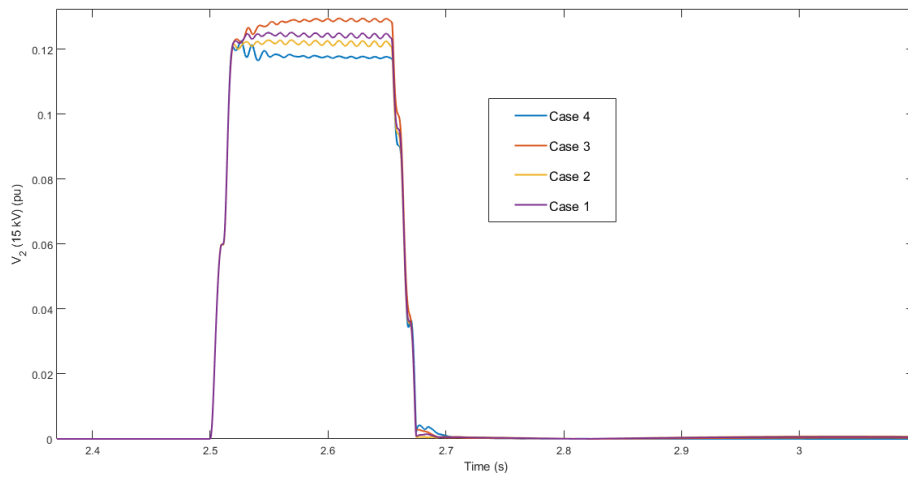


Figure 4.10: Controls comparison,  $V_{2,15}$

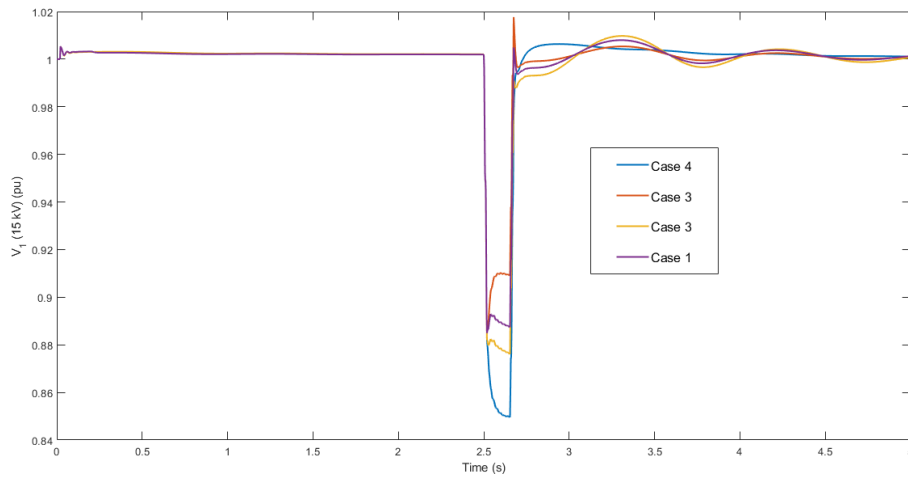


Figure 4.11: Controls comparison,  $V_{1,15}$

As it can be noticed, there is an improvement on the direct sequence voltage dip, however, there is also a small increase in the inverse sequence component. This effect is really small and cannot be avoided if direct current is injected. In addition, for this situation, case 3 (active power priority) seem to be the best option, however, these good results are associated to the fact that  $V_{1,220}$  is really close to  $V_{limit1} = 0.85 pu$ , therefore  $I_p < I_{max}$  and the difference is injected as reactive current. Due to the same effect  $I_q < I_{max}$  when the reactive power is imperative and resultant comparison, as can be shown in 4.13 lead to a higher reactive injection in Case 3. Difference between Case 2 and Case 3 arise for the same effect as explained in the three-phase fault case when  $0.6 < V_{1,220} < 0.85 pu$ .

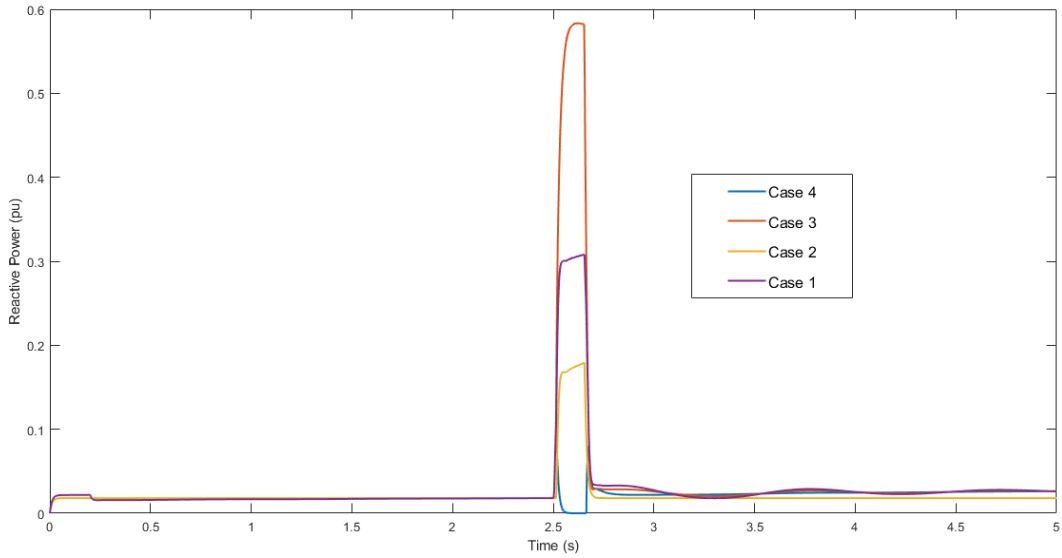


Figure 4.12: Controls comparison, Reactive Power injected by the converter

### 4.2.3 Simple Benchmark

	$V_{220}$ (pu)	$V_{15}$ (pu)	$V_{max,15}$ (pu)	$t_{stab}$ (s)
Case 1	0.4	0.6167	1.022	1.5
Case 2	0.4	0.6167	1.02	1.55
Case 3	0.3112	0.5618	1.031	1.65
Case 4	0.3102	0.559	1.028	1.6

Table 4.8: Experimental  $V_{15}$  and  $V_{220}$ . Simple benchmark.

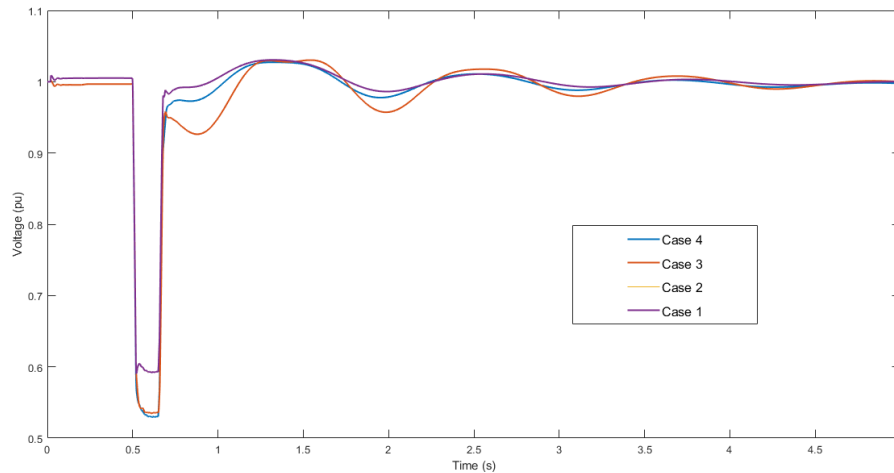


Figure 4.13: Controls comparison, Simple benchmark case

For the purpose of comparing both fault and postfault behaviour of the different controls. As three-phase fault is the disturbance studied  $V_{15}$  and  $V_{220}$  during the fault,  $V_{15,peak}$  once the fault is cleared and time  $t_{stab}$  representing the time it needs to reach  $\pm 1\%$  of the final value, will be obtained. These post-fault values are again chosen for the 15 kV bus.

Due to the lower presence of elements in the grid, fault becomes more critical. However, due to such effect also the impact of the controllers in the grid becomes bigger compared to the case of the complex benchmark.

### 4.3 Theoretical and Experimental Comparison

It is time to compare the results obtained theoretically and through simulations. Below, graphs with both values are shown. Both 15 kV and 220 kV cases are analysed. As it was previously commented, theoretical estimation is based on comparing voltage dips in the controlled system with respect to the non-controlled one. Therefore, these graphs are expressed in  $\Delta V$  in relation to the later system. This comparison only makes sense for the different actions to be done during the fault, hence, Active and Reactive power priority are studied, independently of the control taken during the "normal operation conditions". Figures 4.14 and 4.15 show the comparison according to the influence of the distance to the fault. Figures 4.16 and 4.17 plot the analysis with respect to the influence of the distance from the generator the converter. Finally, Figures 4.18 and 4.19 illustrate the comparison in the frame of different maximum currents allowed.

# Impact of Inverter Based Generation on the Transient Stability Performance of Large Synchronous Power Plants

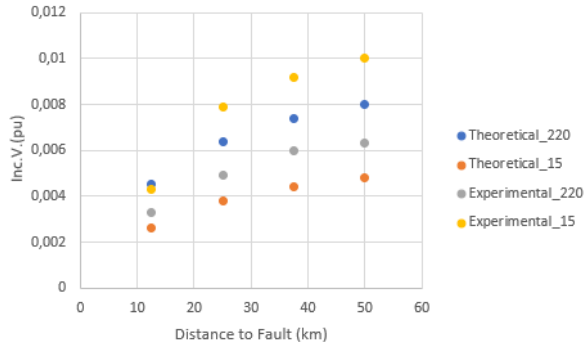


Figure 4.14: Distance to fault influence, Active Power

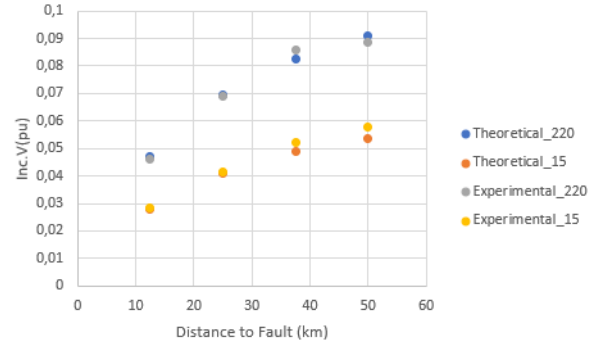


Figure 4.15: Distance to fault influence, Reactive Power

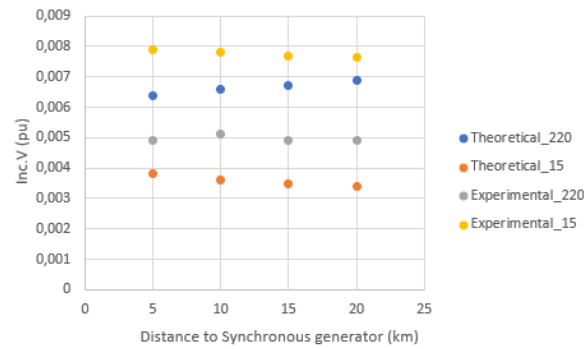


Figure 4.16: Distance to generator influence, Active Power

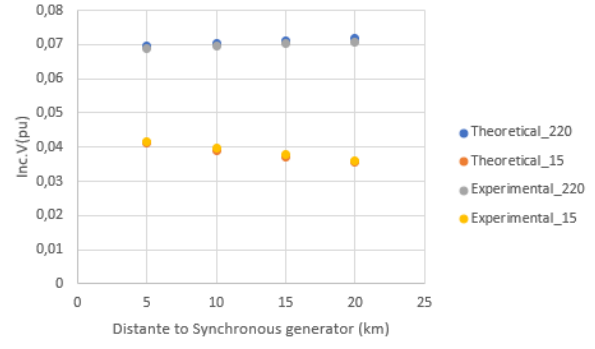


Figure 4.17: Distance to generator influence, Reactive Power

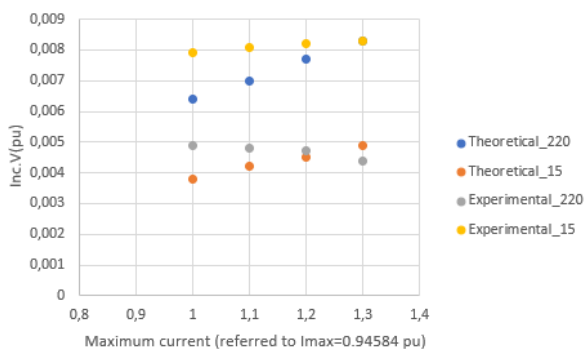


Figure 4.18: Maximum current influence, Active Power

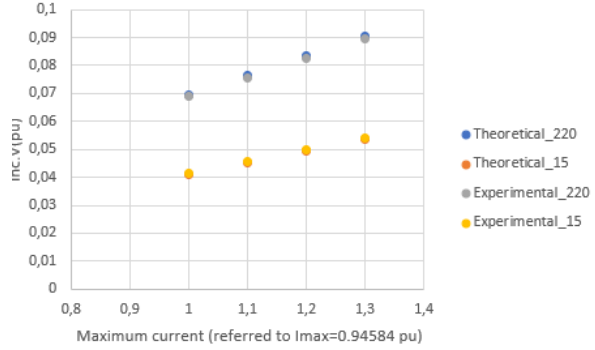


Figure 4.19: Maximum current influence, Reactive Power

From these graphs different conclusions can be obtained.

- Reactive Power priority case perfectly matches the theoretical estimation for the "Distance from converter to generator" and "Maximum current" analysis.
- **Reactive power priority exhibits a slight different behaviour for the longer "Distance to fault" points:** As previously seen, from 37.5 km to fault on, voltage at the 220 kV bus is higher than 0.6 pu during the fault. Therefore, reactive current  $I_q < I_{max}$  and some active current is provided (as it has been seen, its effect is much lower). This makes that  $\Delta V_{effect,theoretical} > \Delta V_{effect,experimental}$  as for the theoretical approach it was assumed that  $I_q = I_{max}$ .
- **Active power priority case is quite different for the theoretical and experimental results:** When the theoretical approach was presented, two main assumptions were taken: extra reactive (resp.active) current due to the losses induced by the active (reactive) power injected during the fault in the reactive (active) priority mode were neglected. In addition,  $\angle \vec{V}_{220}$  was considered the same for subsystem 1 before and after the connection of subsystem 2 so equality for  $I_{d1}$  and  $I_{q1}$  currents was assumed. For the reactive power priority this has no influence, as the  $(\angle \vec{V}_{220})$  remains the same (Figure 4.20) and the extra active current injected does not have much impact. However, for the active power priority case, as it was expected, change in the angle is noticeable (Figure 4.21) and it also can be observed the injection of some more reactive power by the synchronous generators (Figure 4.22). The sum of these effects lead to an increase in the voltage  $V_{15\text{ kV}}$  compared to the theoretical value and a decrease in the  $V_{220\text{ kV}}$  one. These differences are more noticeable as the current injection during the fault is increased (Figure 4.18).

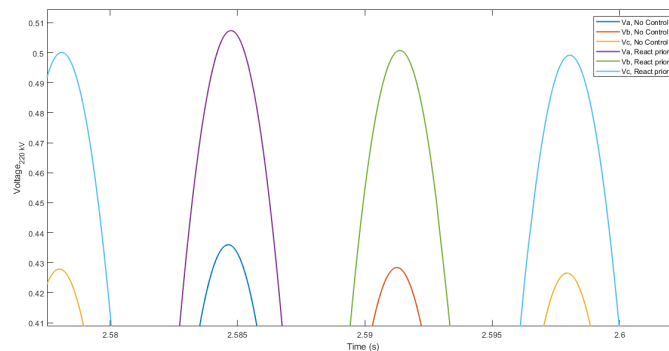


Figure 4.20: Comparison No Control and Reactive priority  $\angle V_{220}$

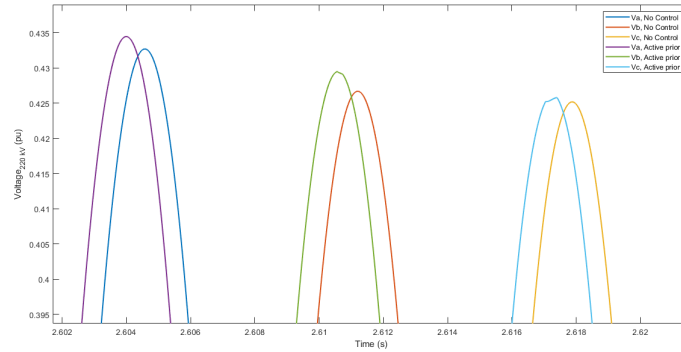


Figure 4.21: Comparison No Control and Active priority  $\angle V_{220}$

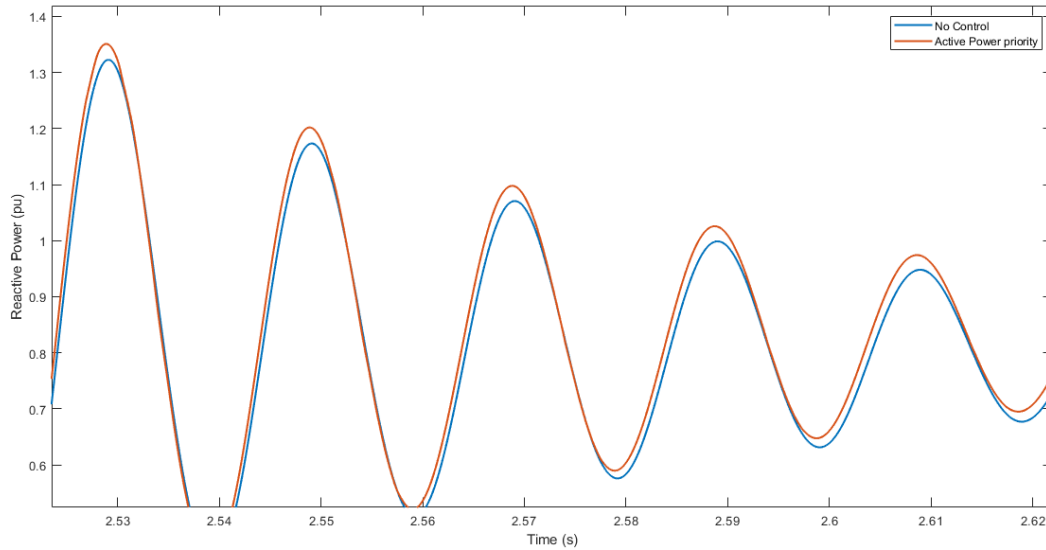


Figure 4.22: Comparison Reactive Power injected by the main synchronous generator in the No Control and Active Power priority situations

Hence, it has been proved, for the reactive power priority case, the good correlation between the theoretical approach and the experimental results. Moreover, for the active power case, results are of the same order of magnitude and explanations for the differences between them have been demonstrated.



# Chapter 5

## Synchronous generator behaviour

In this chapter, influence of the different controls in the machine behaviour will be addressed. In order to do so, following variables are analysed: active current, rotor speed, reactive power and field current. For the sake of conciseness, not all the different situations presented before are going to be analysed here, as machine responses are directly related to the results shown in previous chapter and the analysis would become very rough. The four cases will be compared for 25 km to fault, 5 km to synchronous generator and  $I_{max} = 1.3 \cdot 0.94584 pu$  in order to make the differences more clear. This will be done in the frame of the three phase fault disturbance and the complex benchmark, focusing the comments in the main synchronous generator although comparisons for the case of the non controlled (neither in mechanical input power, nor in Voltage field applied) one will also be done, it is important to notice that these machines have different nominal powers, so exact comparison with the main synchronous generator cannot be done, however what is being sought here is making a qualitative approach of the effect of these controllers in the generator side in the influence of the proposed control modes in the converter as well as the importance of the nominal power of the machine. At the end, one section will be dedicated to possible differences with the case of the SLG fault.

### 5.1 Active Power

As commented in the Introduction chapter, power injected by a synchronous machine, depends, among other variables, on the voltage at the bus where it is connected (Eq. 5.1). Therefore, the higher voltage of the bus, the higher active power the machine is able to provide to the grid. This can be noticed (Figure 5.1) on the behaviour of the active power for cases 1 and 2 (which are coincident) which is capable of injecting much more power than for case 4. However, lower active power of case 3 is due to the fact that some of the active power injected by the converter with this control mode is absorbed by the

synchronous machine, therefore, total contribution is lower. For the postfault situation it can also be observed that the transient of case 3 is the worse and for cases 1 and 2 the best.

Assuming that  $X_d' \approx X_q'$ :

$$P_e = \frac{E' V_s}{X_{total}} \sin(\delta') \quad (5.1)$$

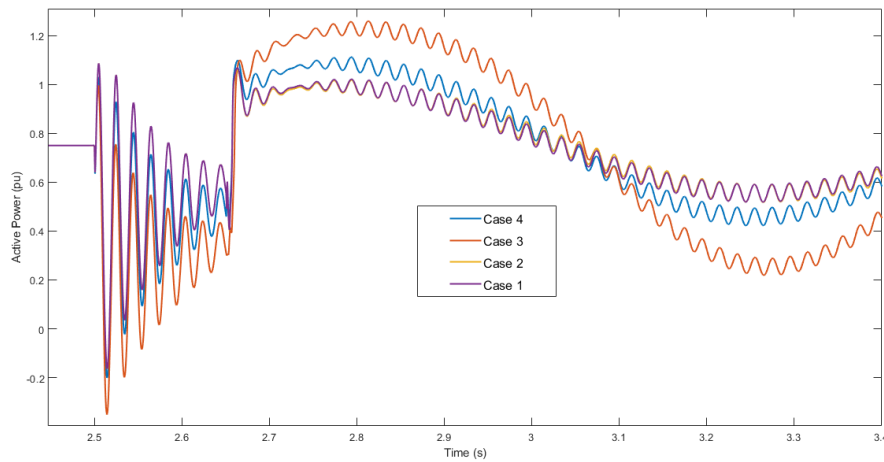


Figure 5.1: Comparison Active Power injected by the main synchronous generator

## 5.2 Rotor Speed

This variable is directly related to the active power (Eq. 5.2) . During the fault, the shaft accelerates due to the unbalance between the input power and the one injected to the grid. So, the lower unbalance, the better. Results show (Figure 5.1) that Case 3 is again the worse one, as lead to higher oscillations in the speed and cases 1 and 2 are the best option regarding the stability of the rotor compared to the non power injection during the fault(case 4). Another useful comparison to be done is the effect of the "Turbine Governor controller" of the generator on the different effects of the controller. It can be observed in Figure 5.3 (Non controlled turbine) that the differences in the rotor speed for the different controls is bigger, and therefore more critical, than for the controlled one (Figure 5.2).

$$P_m - P_e = J \frac{dw}{dt} \quad (5.2)$$

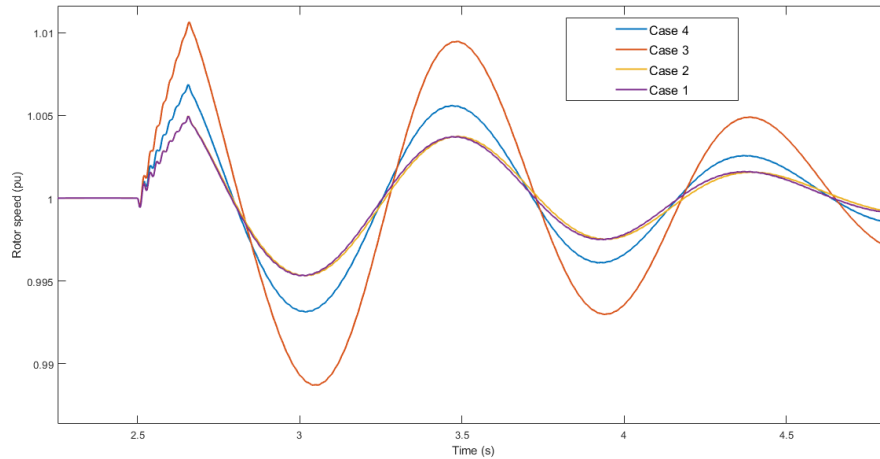


Figure 5.2: Comparison speed of the rotor in the main synchronous generator

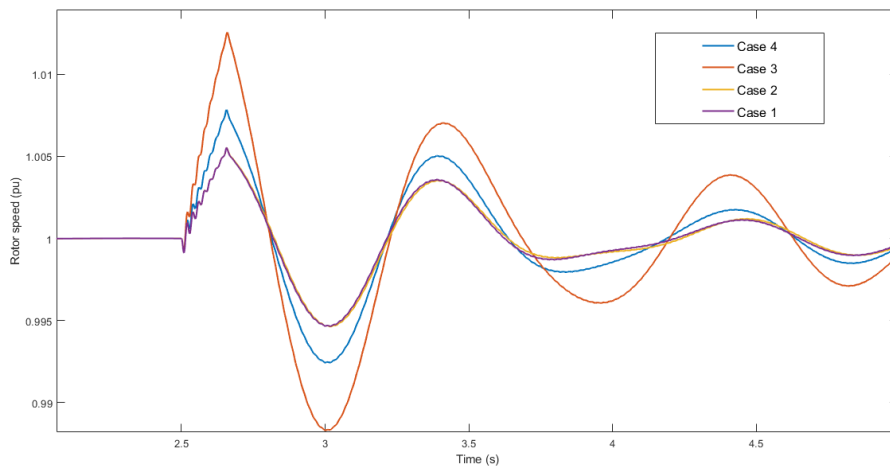


Figure 5.3: Comparison speed of the rotor in the secondary synchronous generator

### 5.3 Reactive Power

This variable is again related to the voltage at the bus. The lower the voltage at the bus, the more reactive current injected into the system. This is confirmed when looking at Figure 5.4, cases 1 and 2 are the ones with higher stator voltage, therefore, lower reactive power. On the other hand, cases 3 and 4 have similar voltages, however, due to previous comments on last chapter, as some more reactive current is needed in the system due to

the reactive losses induced by active current of the converter in case 3, reactive power provided by the machine is higher.

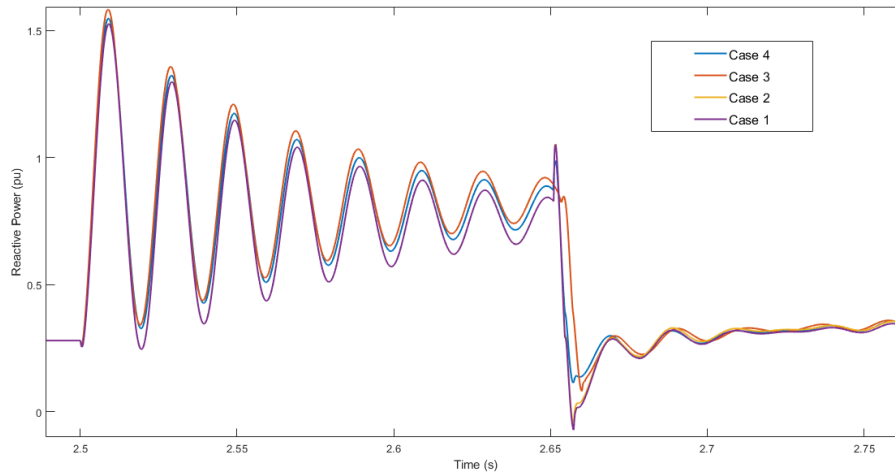


Figure 5.4: Comparison reactive power injected by the main synchronous generator

## 5.4 Field Current

Field current is linked to the current component of the stator in phase with the rotor  $d$  axis. As commented in the introduction chapter, rotor windings oppose to the flux change induced by the high currents flowing into the stator when the disturbance occurs. They act by creating currents in order to overcome this flux change. So, if currents in the stator, and particularly in the  $d$  direction of the rotor, are lower, less screening effect will be induced, so lower field currents will appear. This can be observed in Figure 5.5 where the  $I_d$  currents are plotted for the four different controls proposed, their behaviour is exactly the same, as explained, than the one for the field current (Figure 5.6). For all the three controlled cases, 1,2,3 field current is lower and more or less equal. This can be associated to the fact that active current injected in the system by the machine is quite higher for cases 1 and 2, what compensates somehow the difference with the higher reactive current injected by the generator in case 3. It is also interesting to observe the differences arising from the "Field Voltage Controller", looking at Figure 5.7 (machine with non controlled excitation) it can be noticed that the differences among the control are slightly higher, what makes again, more critical the control action of the converter.

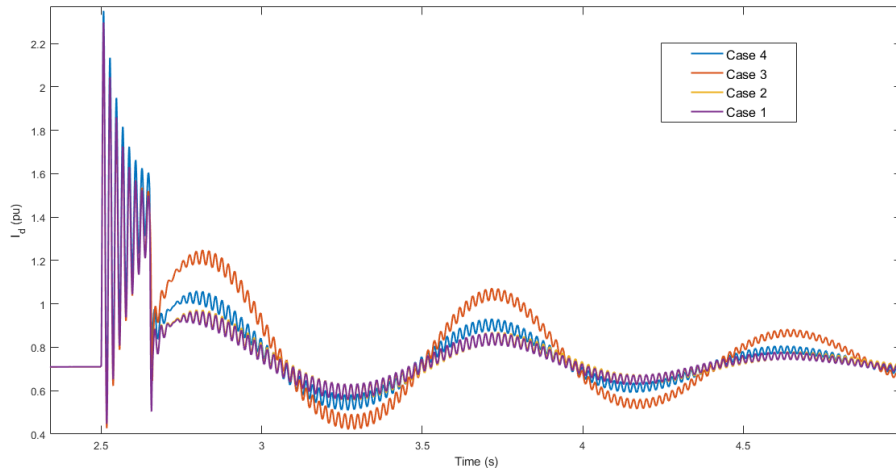


Figure 5.5: Comparison  $I_d$  current in main synchronous generator

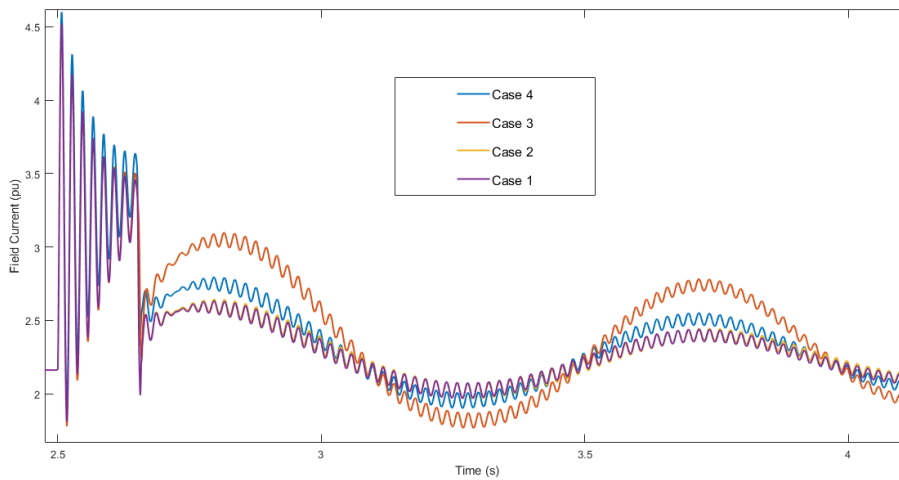


Figure 5.6: Comparison field current in main synchronous generator

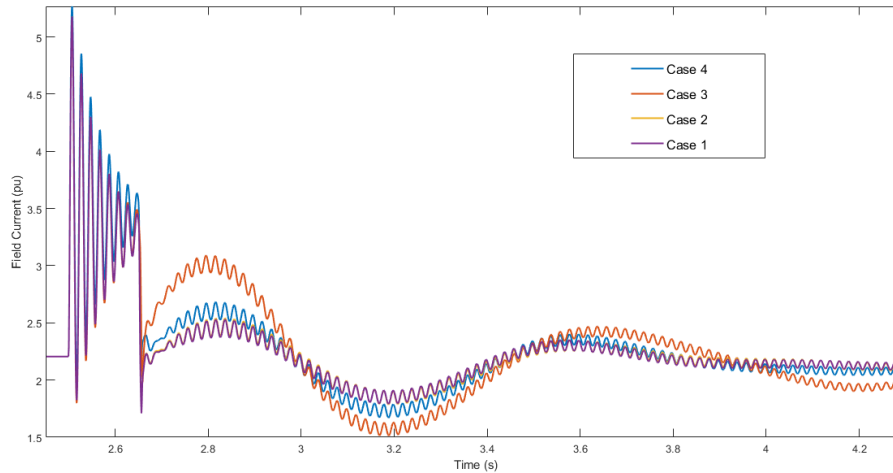


Figure 5.7: Comparison field current in secondary synchronous generator

One important result that has been obtained is the **longer fault clearing time that allows the reactive power priority control**. For the case of 25 km distance to fault, 5 km distance to converter and  $I_{max} = 0.94584$ . Fault clearing time limit is around 450 ms for Case 4 (non controlled) and thanks to the control action, for Case 1 it can reach 750 ms, value which is increased as the maximum current allowed also increase, at makes sense, and it can reach 1 s for  $I = 1.3 \cdot I_{max}$ .

## 5.5 Single Line to Ground Fault

It is also important to comment the situation in the frame of a SLG fault. As it can be seen in Figure 5.8, Active Power injected in case 4 (when  $P = 0$   $Q = 0$  during the fault) is the higher one (in mean value). Despite the fact that other cases lead to higher voltage values (recall Table 4.7) the active power they inject in the system is absorbed partially by the machine, what finally induce a worse behaviour. Especial conditions of the fault ( $V_{1,220}$  close to  $V_{min1} = 0.85$  pu) lead to an active power injected by the converter:

$$0.6(\text{maximum active power allowed}) = P_{Case2} = P_{Case1} > P_{Case3} > P_{Case4} = 0 \quad (5.3)$$

In addition, reactive power injected by Case 2 was lower than for Case 1 (recall Figure 4.22), what makes that slight difference in the active power provided by the machine being a bit higher for Case 1.

Moreover, clearly linked to the active power, is the shape of the rotor speed, as it can be noticed in Figure 5.9 again the best stability case is Case 4, while Case 2 is the worse one.

Finally, related to the field current, it can be observed that the best behaviour (lower values) is presented by Cases 1, 2 and 3 (the controlled ones), they are quite close but the lowest transient is associated to Case 3. This effect is associated again to the highest reactive power injected by the converter in this situation during the fault, and hence, higher voltage at the 15 kV bus.

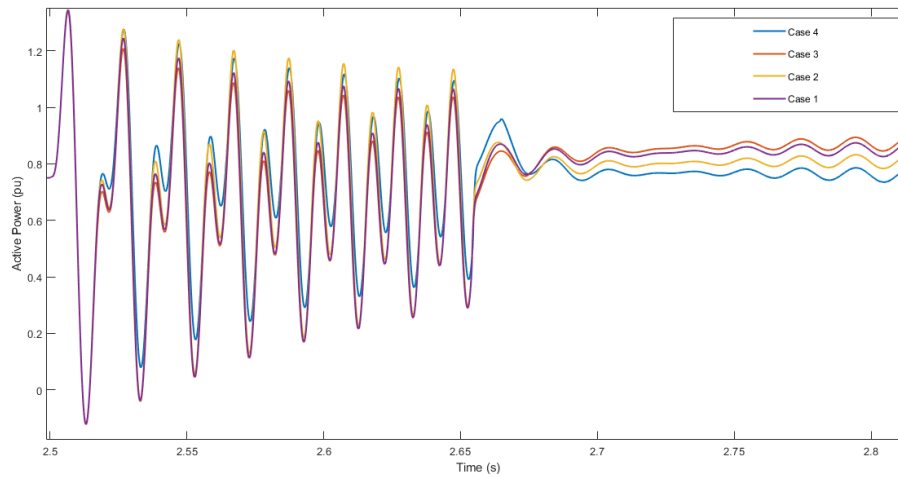


Figure 5.8: Comparison Active power injected by the main synchronous generator during SLG

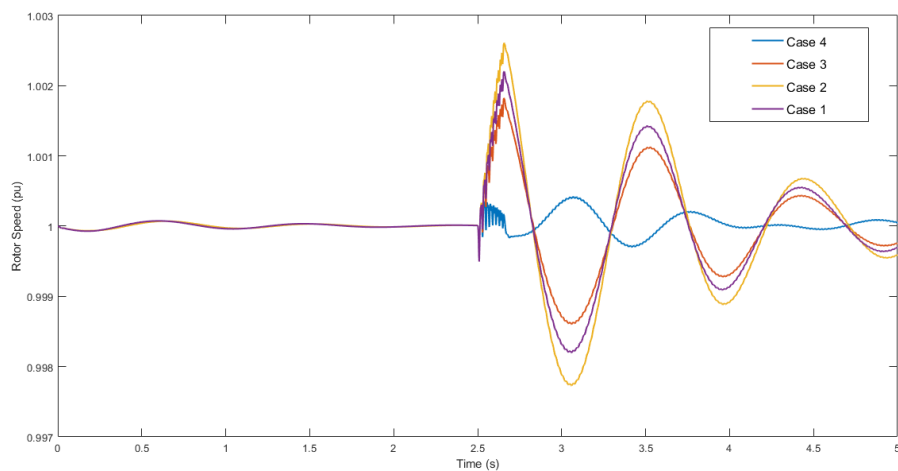


Figure 5.9: Comparison rotor speed in main synchronous generator during SLG

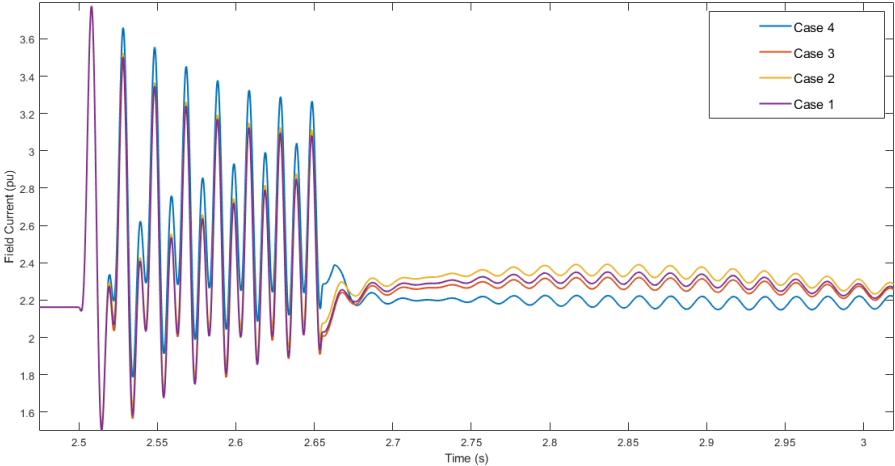


Figure 5.10: Comparison field current in main synchronous generator during SLG

# Chapter 6

## Conclusions

Finally, it is now time to summarize and concentrate all the conclusions that can be extracted from this document. As it has been repeated several times along the text, the aim of this work is trying to identify the effect of the inverter based generation on the transient behaviour of synchronous power plants. Inverter based generation is considered as coming from two different sources, namely HVDC links and Power Park modules. These conclusions can be divided into the following topics, which follows approximately the structure of the document:

- Regulatory frame
- Modeling of the converter
- Validity of the results
- Effect of the controllers on the voltage
- Effect of the controllers on the synchronous generator behaviour
- Overall analysis of each model proposed

### **Regulatory Frame**

First of all, actual regulatory frame in the European Union for the connection of HVDC links and Power Park modules has been studied. This legislation establish the main guidelines to be accomplished, however, it does not set a specific way to implement them. Each national Grid Operator is in charge of this task. Therefore, Belgian and Spanish documents regarding this topic have been analysed in order to make realistic the different

actions to be done on the converters and to be conscious about the constraints that must be fulfilled. Two main ideas arise from their reading, controls to be applied on the converter depend on the grid voltage at the bus where it is connected, and main actions during fault circumstances are related to the priority given to the active or the reactive power injection.

They can be classified as follows:

- **Normal Operation Conditions:**

- Reactive Power Control
  - \* Reference Reactive Power Control Mode
  - \* Voltage Control Mode
- Active Power Control
  - \* Limited frequency sensitive mode overfrequency
  - \* Limited Frequency sensitive mode underfrequency
  - \* Frequency Sensitive mode

- **Faulty conditions**

- Reactive Power priority
- Active Power priority

These controllers can also be applied during unbalance disturbances, with the option of injecting direct and inverse sequence currents depending on the case.

### **Modeling of the converter**

Common real converters are based on DC/AC interfaces which play on the voltage that must be applied in order to generate the desired currents, which are obtained from the voltage at the bus where the converter is connected and the reference active and reactive powers coming from the controllers aforementioned. These devices need from a control loop in order to check that the currents injected are effectively the ones calculated. Moreover, due to their working principle they will create some harmonic distortion that is undesirable in the system. For the purpose of this work, transient stability behaviour, according to [8], the converter can be simulated using RMS model, where it is represented through three controlled current sources, one for each phase, where a logic controller establish their value and, due to the high switching frequency of the device (frequency of the inner loop managing the current) compared to the time frame of the stability purposes, it

can be considered to follow instantaneously the reference value. Moreover, based upon the same reason, harmonic distortion is neglected and final currents are perfectly sinusoidal.

### Validity of the results

In order to compare the effect of the controls mentioned in the national grid codes, 4 different models (cases) are developed. First two of these cases are dedicated to the analysis of the Reactive Power Control mode during normal operation conditions. In addition, the third case has the aim of comparing the power priority effect during the fault. And lastly, in order to verify their general contribution, one final case is built where neither active nor reactive power is injected by the converter during the fault. Active Power control modes are not compared because the frequency deviation is quite low (Figure 4.5), therefore, for the sake of conciseness it does not make sense to do develop another case just for this slight difference.

These models have been developed in the frame of a three-phase fault, as it is the most critical situation for the stability of the machine. However, other unbalanced disturbances are more common in the grid. Therefore, SLG fault case is also analysed and ,according to [9] the best strategy consists in not injecting inverse sequence currents, what lead to the possibility of using the same controllers for that disturbance.

In order to ensure the validity of the results coming from *Matlab/Simulink* models representing these 4 cases studied, a theoretical approach is sought. This approach is based upon comparing the voltage dip during a three-phase fault at the two most important buses of the system , the 15 kV (synchronous generator bus) and the 220 kV (converter bus) one, with respect to the case where neither active nor reactive power is injected during the fault (Case 4) using kind of a superposition principle, where the global system is divided into two subsystems and the converter is "isolated" into the second one.

From this theoretical and experimental analysis, following conclusions can be extracted:

- Reactive Power priority during the fault matches perfectly the theoretical approach with the experimental results. Except for the situations when the voltage at the converter bus is higher than  $V = 0.6 pu$ . In these cases, due to the working principle of the controllers, some active power is injected what invalidates the assumption of  $I_q = I_{max}$  in the converter.
- Active Power deviates from the theoretical estimation. Despite the fact that results are of the same order of magnitude some clear differences can be observed. Explan-

ation for this phenomenon has been deduced. Firstly, it is not possible to isolate the action of the converter independently from the other electrical sources of the system (generators and electrical grids) due to the fact that in the Active power priority case some reactive losses will be induced in the reactances present in the system and they need to be compensated by some "extra" injection in these sources. Same effect occurs for the Reactive power priority case, however, this lead to "extra" active power flowing in the system, which does not influence a lot in the results. In addition, for the theoretical approach,  $d, q$  frame associated to the 220 kV bus is used. Therefore, if associated to the power injection of the converter there is a change in  $\angle \overrightarrow{V_{220 \text{ kV}}}$ , real case deviates from the assumption done in the theoretical estimation and results will be distorted. Active power injection leads to a change in this angle, however, reactive power injection keeps essentially the same phase, as it is demonstrated.

Therefore, experimental results are validated. This ensures the correct functioning of the converter and that the effect they cause is the one expected from a theoretical point of view.

### **Effect of the power injected by the controllers on the voltage**

Once the results have been validated it is time to show the conclusions about their effect on the system:

- Reactive Power injection during the fault lead to lower voltage dips, and therefore, to a better behaviour of the system.
- Active Power injection has a really low effect in the voltage dip.
- Effect of the controllers is also related to three important parameters: distance from the converter to the fault, distance from the converter to the synchronous generator and maximum current allowed by the converter during the disturbance. The higher distance to the fault, and the higher maximum current, the higher effect on both 220 kV and 15 kV bus. However, the higher distance to the synchronous generator has a slightly higher effect on the 220 kV but a lower on the 15 kV one.
- The most critical is the situation, the lower elements presents in the grid and the lower loads lead to a higher effect of the controller, as it was deduced from the Simple benchmark model.

### Effect on the synchronous generator

Four variables are studied:

- **Active Power:** The higher reactive power injected by the converter, the higher voltage at the generator bus, as it has been explained. Therefore, converter reactive power injection allows to increase the active power injection capability of the generator during the fault. On the other side, if active power is injected through the converter, part of this amount will be absorbed by the rotor shaft, what is undesirable for the stability purpose.
- **Rotor Speed:** this variable is linked to the active power injected by the generator during the fault. The higher it is, the lower difference with the incoming mechanical power and therefore, the lower increase in the rotor of the shaft.
- **Reactive Power:** the higher voltage at the generator bus, the lower reactive power injected. Therefore, increasing reactive current injection by the converter leads to an increasing voltage and a decreasing reactive power injection by the machine. In addition it has to be also taken into account the comment on the "extra" reactive power provided by the generator when the converter injects active power in the system.
- **Field Current:** this variable is associated to the  $d$  component of the stator current. As explained in the introduction, due to the *Constant flux linkage principle* the higher flux generated in the  $d$  axis of the stator the higher field current induced.

### Overall analysis of each controlled proposed

As it has been commented, and clearly seen, reactive power injection during the fault has the best effect on the system and on the generator behaviour. However, active power has an undesirable unstability effect on the machine.

Based on these principles, reactive power priority is clearly the best option during fault situations. Cases 1 and 2 exhibited the most stable behaviour. This is truth for all of the three-phase fault cases analysed, however, for SLG cases active power priority showed better results. This is associated to the construction of the "Active Power priority (Case 3)" controller and the value of  $V_{1,220} \text{ kV}$  in the SLG case. For high values of  $V_{1,220} \text{ kV}$ , close to  $V_{min1} = 0.85 \text{ pu}$ , active power injected in "Case 3" is not too high (due to  $\Delta I_r$  is low) therefore, in order to fulfill the constraint of  $I = I_{max}$ , much reactive power is injected. However, for Cases 1 and 2, the closeness between  $V_{1,220}$  and  $V_{min1}$  results in low reactive power injected. Therefore, this result which was associated to SLG fault, will also occur

if the distance from the fault to the converter is high enough to make  $V_{220}$  near to  $V_{min1}$ .

It can also be noticed that for the synchronous stability of the machine, active power injection during the fault is not a good choice, as part of this injection will be absorbed by the rotor shaft what tends to increase its kinetic energy and lead to more risky behaviour. However, for the rest of the system is a good option as it is necessary to have active power injection which feeds the different loads present in the grid and avoid somehow their disconnection, although it is necessary to take care about the amount of power injected, as many loads are passive ones and if the voltage is not high enough they could not absorb all the desired power, what may cause really high currents flowing along the overhead lines. In addition, active power consumption during the fault, what would be better for the stability of the synchronous generator, is quite risky as if the genertor elements on the grid are not capable (due to the voltage dip) to provide this energy, important problems could occur in the converter.

It is also important to note that this active power priority case here developed does not come from any grid code, it has been personally created, by comparing it with the reactive power priority one, in order to analyse its possible effect. Therefore, other more useful controls could exist.

Now, comparing Cases 1 and 2, the following comments can be done. Along the document, most of the situations lead to a  $V_{220} < V_{min2} = 0.6 pu$ , therefore, in accordance to the working principle of the controller, same reactive power was injected and during this situation did not exist any differences (only if reactive power for both cases were different previously to the fault, and comments to this fact were already done). However, for many situations (if the fault is far enough) this would not be the case and the behaviour of the Voltage control mode (Case 1) demonstrates to be better, as it can adapt itself to the change. In addition, regarding the postfault situation, voltage control mode exhibits a quicker and less sharp behaviour. Disadvantage of this control could be the undesirable interaction with other controllers, however, as a limitation is always set in the reactive power values, this effect would not be too high.

In addition, one really important effect is the longer clearing time allowed when reactive power is injected during the fault.

From all these comments, one idea has arised in order to improve the working principle of the system. Make one mix where, for high voltage dips, reactive power is the imperative power and, in the case of lower voltage dips, active power could be the best option.

# Bibliography

- [1] J. Machowski, J.W. Bialek, and J. Bumby. *Power System Dynamics: Stability and Control*. Wiley, 2011.
- [2] IEA(2019). Renewables 2019. Technical report, IEA, 2019. <https://www.iea.org/reports/renewables-2019>.
- [3] Emmanuel de Jaeger. *Wind Energy Conversion*. LELEC2753-Ecole Polytechnique de Louvain, 2020.
- [4] Emmanuel de Jaeger. *Flexible AC Transmission Systems*. LELEC2753-Ecole Polytechnique de Louvain, 2020.
- [5] The European Comission. Comission regulation (eu) 2016/1447. *Official Journal of the European Union*, 2016.
- [6] Red Electrica de España. Requisitos tecnicos mínimos de conexión de sistemas hvdc y módulos de parque eléctrico conectados en corriente continua. Technical report, Red Eléctrica de España, 2018.
- [7] Elia. Proposal for nc rfg requirements of general application. Technical report, Elia, 2018.
- [8] K. Yamashita, H. Renner, S. Martínez Villanueva, G. Lammert, P. Aristidou, J. Carvalho Martins, L. Zhu, L. D. Pabón Ospina, and T. Van Cutsem. Industrial recommendation of modeling of inverter-based generators for power system dynamic studies with focus on photovoltaic. *IEEE Power and Energy Technology Systems Journal*, 5(1):1–10, 2018.
- [9] H. Aji, M. Ndreko, M. Popov, and M. A. M. M. van der Meijden. Investigation on different negative sequence current control options for mmc-hvdc during single line to ground ac faults. In *2016 IEEE PES Innovative Smart Grid Technologies Conference Europe (ISGT-Europe)*, pages 1–6, 2016.

## BIBLIOGRAPHY

---

- [10] Emmanuel de Jaeger. *Voltage Control*. LELEC2520-Ecole Polytechnique de Louvain, 2019.

# List of Figures

1.1	Armature flux paths in the different transient states, (a) subtransient, (b) transient, (c) steady state . . . . .	4
1.2	Armature reactances in the different transient states, (a) subtransient, (b) transient, (c) steady state . . . . .	5
1.3	Emf in the different transient states . . . . .	6
1.4	Active power balance in a three-phase fault close to the generator . . . . .	8
1.5	$P_{E'}(\delta')$ depending on the kind of fault, when close to the generator . . . . .	9
1.6	Comparison of costs for HVDC and AC transmission systems in function of the distance . . . . .	11
1.7	Control strategy applied in a Voltage source inverter . . . . .	12
2.1	Reactive Power capability in extreme voltage ranges . . . . .	14
2.2	Frequency sensitive mode scheme . . . . .	15
2.3	Frequency sensitive mode parameters . . . . .	15
2.4	Additional reactive current when reactive power is imperative . . . . .	16
3.1	Control Scheme of the converter . . . . .	24
3.2	Scheme of voltage control mode . . . . .	26
3.3	Scheme of prior reactive power control mode . . . . .	29
3.4	Scheme of prior active power control mode . . . . .	30
3.5	Simple Benchmark . . . . .	31
3.6	Complex Benchmark . . . . .	32
4.1	Subsystem 1 . . . . .	38
4.2	Subsystem 2 . . . . .	38
4.3	Control Comparison, 25 km to fault, 5 km to generator and $I_{max} = 0.94584$ . . . . .	43
4.4	Case 1, Distance to fault influence . . . . .	43
4.5	Frequency of the grid at the connection point of the converter . . . . .	43
4.6	Controls comparison, 25 km to fault and 5 km to synchronous generator . . . . .	44
4.7	Case 1, Maximum current influence . . . . .	45

## LIST OF FIGURES

---

4.8	Controls comparison, Distance converter to generator influence . . . . .	46
4.9	Reactive Power control comparison for different references . . . . .	47
4.10	Controls comparison, $V_{2,15}$ . . . . .	48
4.11	Controls comparison, $V_{1,15}$ . . . . .	48
4.12	Controls comparison, Reactive Power injected by the converter . . . . .	49
4.13	Controls comparison, Simple benchmark case . . . . .	50
4.14	Distance to fault influence, Active Power . . . . .	51
4.15	Distance to fault influence, Reactive Power . . . . .	51
4.16	Distance to generator influence, Active Power . . . . .	51
4.17	Distance to generator influence, Reactive Power . . . . .	51
4.18	Maximum current influence, Active Power . . . . .	51
4.19	Maximum current influence, Reactive Power . . . . .	51
4.20	Comparison No Control and Reactive priority $\angle V_{220}$ . . . . .	52
4.21	Comparison No Control and Active priority $\angle V_{220}$ . . . . .	53
4.22	Comparison Reactive Power injected by the main synchronous generator in the No Control and Active Power priority situations . . . . .	53
5.1	Comparison Active Power injected by the main synchronous generator . . .	56
5.2	Comparison speed of the rotor in the main synchronous generator . . . . .	57
5.3	Comparison speed of the rotor in the secondary synchronous generator . .	57
5.4	Comparison reactive power injected by the main synchronous generator . .	58
5.5	Comparison $I_d$ current in main synchronous generator . . . . .	59
5.6	Comparison field current in main synchronous generator . . . . .	59
5.7	Comparison field current in secondary synchronous generator . . . . .	60
5.8	Comparison Active power injected by the main synchronous generator dur- ing SLG . . . . .	61
5.9	Comparison rotor speed in main synchronous generator during SLG . . . .	61
5.10	Comparison field current in main synchronous generator during SLG . . .	62

# List of Tables

3.1	Generator Parameters . . . . .	20
3.2	Secondary Generator Parameters . . . . .	21
4.1	Theoretical approach.Distance to fault influence . . . . .	41
4.2	Theoretical approach. Distance to synchronous generator influence . . . . .	41
4.3	Theoretical approach. Maximum allowed current by the converter influence	41
4.4	Experimental $V_{15}$ and $V_{220}$ . Distance to fault influence. . . . .	42
4.5	Experimental $V_{15}$ and $V_{220}$ . Maximum Current influence. 25 <i>km</i> to fault and 5 <i>km</i> to generator . . . . .	44
4.6	Experimental $V_{15}$ and $V_{220}$ . Distance to generator influence . . . . .	45
4.7	Experimental $V_{15}$ and $V_{220}$ . SLG fault. . . . .	48
4.8	Experimental $V_{15}$ and $V_{220}$ . Simple benchmark. . . . .	49

UNIVERSITÉ CATHOLIQUE DE LOUVAIN  
École polytechnique de Louvain

Rue Archimède, 1 bte L6.11.01, 1348 Louvain-la-Neuve, Belgique | [www.uclouvain.be/epl](http://www.uclouvain.be/epl)